

000 001 002 003 004 005 006 007 008 009 010 011 012 013 014 015 016 017 018 019 020 021 022 023 024 025 026 027 028 029 030 031 032 033 034 035 036 037 038 039 040 041 042 043 044 045 046 047 048 049 050 051 052 053 SAFETY-ALIGNED WEIGHTS ARE NOT ENOUGH: REFUSAL-TEACHER-GUIDED FINETUNING EN- HANCES SAFETY AND DOWNSTREAM PERFORMANCE UNDER HARMFUL FINETUNING ATTACKS

008 **Anonymous authors**

009 Paper under double-blind review

012 ABSTRACT

014 Recently, major AI providers such as Google and OpenAI have introduced
015 Finetuning-as-a-Service (FaaS), which allows users to customize Large Language
016 Models (LLMs) using their own data. However, this service is vulnerable to safety
017 degradation when user data includes harmful prompts, a threat known as harmful
018 finetuning attacks. Prior works attempt to mitigate this issue by first constructing
019 safety-aligned model and then finetuning the model on user data. However, we ob-
020 serve that the safety-aligned weights provide weak initialization for downstream
021 task learning, leading to suboptimal safety-alignment and downstream task per-
022 formance. To address this, we propose a **Refusal-Teacher (Ref-Teacher)-guided**
023 **finetuning framework**. Instead of finetuning a safety-aligned model on user data,
024 our approach directly finetunes the base model under the guidance of a safety-
025 aligned Ref-Teacher, which filters harmful prompts from user data and distills
026 safety-alignment knowledge into the base model. Extensive experiments demon-
027 strate that our Ref-Teacher-guided finetuning strategy effectively minimizes harm-
028 ful outputs and enhances finetuning accuracy for user-specific tasks, offering a
029 practical solution for secure and reliable deployment of LLMs in FaaS.

031 1 INTRODUCTION

033 Recent advancements in Large Language Models (LLMs) (Touvron et al. (2023); Jiang et al. (2023);
034 Team et al. (2024); Team (2024); Hurst et al. (2024); Guo et al. (2025); Research et al. (2025)) have
035 achieved remarkable performance across a wide range of natural language processing tasks. LLMs
036 are typically pretrained on massive and diverse corpora, resulting in strong generalization ability and
037 broad applicability across domains. To further facilitate LLMs for individual and domain-specific
038 purposes, major AI service providers such as Google and OpenAI offer not only access to pretrained
039 LLMs but also Finetuning-as-a-Service (FaaS). This service enables users to upload custom datasets
040 and adapt LLMs to more specific tasks and domains depending on their unique requirements.

041 However, FaaS must prevent the malicious use of LLMs through safety-alignment, even when users
042 attempt to jailbreak the models via customization. These types of attacks, which inject harmful
043 prompts into user data for finetuning, are called *harmful finetuning attacks*. Several studies (Qi et al.
044 (2023); Lermen et al. (2023); Rosati et al. (2024); Huang et al. (2024b;c;d); Li et al. (2025); Huang
045 et al. (2025)) have shown that finetuning on user data containing harmful content compromises
046 the safety-alignment, despite the LLMs being safety-aligned before finetuning. This vulnerability
047 highlights the need to preserve safety while achieving high performance on user tasks in FaaS.

048 To mitigate these risks, prior works typically adopt a two-stage pipeline. In the first stage, referred
049 to as the *alignment stage*, pretrained LLMs are trained on safety-alignment data to avoid generating
050 harmful responses. In the second stage, referred to as the *finetuning stage*, the safety-aligned models
051 are finetuned on user data for user-specific downstream tasks. Within this pipeline, some methods
052 find robust model weights against harmful finetuning attacks during the alignment stage (Huang
053 et al. (2024c;d); Liu et al. (2024); Rosati et al. (2024)), while others preserve safety-aligned weights
054 during the finetuning stage (Mukhoti et al. (2023); Huang et al. (2024b); Li et al. (2024a; 2025)).

054 However, we observe that the two-stage pipeline adopted in prior works is suboptimal. Safety-
 055 aligned models provide weak weight initialization for learning downstream tasks, resulting in limited
 056 task performance and compromised safety. A more effective alternative is to directly finetune the
 057 base model on both user data and safety-alignment data during finetuning stage, thereby enhancing
 058 downstream task performance while preserving safety. Nevertheless, this base model finetuning
 059 strategy suffers from gradient conflicts between the two objectives, safety and user task, which
 060 destabilize training and are further exacerbated when user data contains harmful prompts.

061 Building on these observations, we propose a novel **Refusal-Teacher (Ref-Teacher)-guided fine-**
 062 **tuning framework** (Fig. 1), which directly finetunes the base model on both user data and safety-
 063 alignment data under the guidance of a Ref-Teacher. In our framework, the Ref-Teacher serves two
 064 complementary roles. First, it performs **Alignment Distillation** by generating soft refusal labels that
 065 provide richer supervision and yield smoother loss surfaces, thereby mitigating gradient conflicts.
 066 Second, it performs **Data Filtering** by removing harmful prompts from user data based on its refusal
 067 feature, ensuring robust conflict mitigation against harmful finetuning attacks. Through these two
 068 roles, our framework effectively alleviates gradient conflicts, which in turn enables improved safety
 069 and downstream task performance even under harmful finetuning attacks.

070 Our extensive experiments demonstrate the effectiveness of the Ref-Teacher-guided finetuning
 071 framework in enhancing both user-specific task performance and safety-alignment. Across a wide
 072 range of evaluations, our method consistently achieves the highest finetuning accuracy and the low-
 073 est harmful scores compared to all baselines. Consequently, our framework overcomes the limita-
 074 tions of prior two-stage pipelines and offers a practical solution for secure and reliable FaaS.

075 Our Contributions.

- 076 • We demonstrate that safety-aligned LLMs provide weak initialization for downstream learning,
 077 resulting in suboptimal task performance and compromised safety, whereas directly finetuning the
 078 base model on safety-alignment data and user data improves both safety and task performance.
- 079 • However, this base model finetuning strategy suffers from gradient conflicts between safety and
 080 user task objectives, which are further exacerbated when user data includes harmful prompts.
 081 To overcome this, we propose the Refusal-Teacher(Ref-Teacher)-guided finetuning framework,
 082 which mitigates such conflicts through (i) alignment distillation and (ii) data filtering.
- 083 • Extensive experiments demonstrate that our framework achieves strong performance on user-
 084 specific downstream tasks while consistently preserving safety across diverse settings.

086 2 RELATED WORKS

088 **Safety in Large Language Models.** Large Language Models (LLMs) can respond to diverse queries
 089 but are vulnerable to harmful prompts (Ji et al. (2023); Zou et al. (2023)), which can elicit unsafe
 090 outputs such as weapon-making instructions. To mitigate these risks, safety-aligned LLMs (Team
 091 (2024); Llama Team (2024); Team et al. (2024)) have been developed, trained via Supervised Fine-
 092 Tuning (Bianchi et al. (2023)) or Reinforcement Learning with Human Feedback (Ouyang et al.
 093 (2022); Rafailov et al. (2023)) on datasets that pair harmful prompts with refusal responses, en-
 094 abling them to reject unsafe requests. Nevertheless, they remain vulnerable to advanced jailbreaking
 095 techniques (Chao et al. (2023); Liu et al. (2023); Zou et al. (2023); Li et al. (2024b)). Training-free
 096 defenses leverage LLMs’ ability to assess harmfulness (Wang et al. (2024); Zhang et al. (2024)),
 097 or exploit internal differences when processing harmful versus harmless inputs (Xie et al. (2024);
 098 Hu et al. (2024); Hung et al. (2024)). In contrast, training-based methods enhance robustness by
 099 finetuning LLMs through adversarial training. Some approaches adjust the balance of harmful and
 100 harmless prompts (Bianchi et al. (2023)), while others generate adversarial samples via latent-space
 101 perturbations (Sheshadri et al. (2024a;b); Xhonneux et al. (2024); Zou et al. (2024); Yu et al. (2024)).

102 Other methods train separate safe and unsafe models and apply safe decoding strategies Banerjee
 103 et al. (2025); Du et al. (2024); Xu et al. (2024); Zhao et al. (2024). Recently, the concept of a refusal
 104 feature, which encodes the refusal behavior of safety-aligned LLMs, is introduced, leveraging it in
 105 both adversarial attacks Ardit et al. (2024) and defense Yu et al. (2024). Building on the insight
 106 of the refusal feature, we further analyze the refusal feature and demonstrate its effectiveness in
 107 classifying prompts as harmful or harmless. Based on the capability of refusal feature, we propose
 a novel finetuning strategy for safe LLM finetuning.

108 **Defending Harmful Finetuning Attacks.** Harmful finetuning attacks are a subclass of jailbreaking
 109 techniques in which harmful input-output pairs are injected into the finetuning data, leading
 110 the model to generate unsafe outputs. The risks associated with harmful content in finetuning data
 111 have been highlighted in several studies (Lermen et al. (2023); Qi et al. (2023); Zhan et al. (2023);
 112 Hsu et al. (2024); He et al. (2024); Poppi et al. (2024); Betley et al. (2025); Hsiung et al. (2025);
 113 Xiao et al. (2025)). This makes preserving safety-alignment against harmful finetuning attacks in-
 114 creasingly critical, especially as AI providers begin offering FaaS. To address this issue, prior works
 115 proposed solutions targeting the alignment stage, the finetuning stage, or the post-finetuning stage.
 116 First, alignment-stage solutions aim to obtain robust safety-aligned LLM weights against harm-
 117 ful finetuning attacks, typically through regularization techniques based on expected perturbations
 118 (Huang et al. (2024c;d); Liu et al. (2024); Rosati et al. (2024); Tamirisa et al. (2024)). Second,
 119 finetuning-stage solutions preserve safety during finetuning on user data by freezing safety-critical
 120 parameters (Li et al. (2024a); Wei (2024); Li et al. (2025)) or incorporating safety regularization
 121 (Mukhoti et al. (2023); Huang et al. (2024b); Qi (2024); Yang et al. (2025)), often with additional
 122 safety-alignment data as guidance. Lastly, post-finetuning-stage solutions analyze differences be-
 123 tween safety-aligned and finetuned models, and then edit model weights to compensate for safety
 124 degradation (Huang et al. (2024a); Hsu et al. (2024); Yi et al. (2025)).

125 Beyond these methods, recent works have examined how feature-space similarity. Hsiung et al.
 126 (2025) shows that safety guardrails weaken when downstream data representations overlap with
 127 safety-alignment data, while Xiao et al. (2025) reveals that benign prompt styles applied to harmful
 128 inputs can bypass safety mechanisms. Both findings relate to our refusal-feature-similarity-based
 129 filtering, which also addresses feature-level similarity between harmful and benign data.

130 In contrast to prior works following two-stage pipeline, we propose a Refusal-Teacher (Ref-
 131 Teacher)-guided finetuning framework, which directly finetunes the base model under the guidance
 132 of the Ref-Teacher, achieving better performance in both safety and downstream tasks.

133 3 PROBLEM SETTING

136 **Scenario.** In Finetuning-as-a-Service (FaaS), AI providers pursue two primary objectives: (i)
 137 achieving high user-specific task performance and (ii) preserving the safety-alignment of customized
 138 LLMs. To address these goals, we consider two distinct phases: the *alignment stage* (service prepa-
 139 ration) and the *finetuning stage* (service provision). In the alignment stage, service providers are
 140 assumed to have access to a dataset of 5,000 harmful prompts and 5,000 harmless prompts, where
 141 each harmful prompt is paired with a refusal response. In the finetuning stage, users submit custom
 142 datasets to the provider for LLM customization. Importantly, providers have neither prior knowledge
 143 of whether user data contains harmful prompts nor its distribution during the alignment stage.

144 **Threat Models.** We assume that user data contains $p\%$ harmful prompts with harmful responses,
 145 while the remaining $(1 - p)\%$ consists of harmless prompts sampled from the same dataset. When
 146 $p = 0$, the dataset includes only harmless prompts. Importantly, users do not inform which prompts
 147 are harmful or harmless, thereby exposing LLMs to the risk of safety degradation during finetuning.
 148 At the same time, LLMs are expected to achieve strong performance on user-specific downstream
 149 tasks while preserving their safety-alignment, making the problem particularly challenging.

150 4 MOTIVATION: SAFETY-ALIGNED WEIGHTS ARE NOT ENOUGH.

153 Prior works on defending against harmful finetuning attacks have adopted a two-stage pipeline:
 154 first performing safety-alignment on an LLM, and then finetuning the safety-aligned model on user
 155 data. However, we find this paradigm suboptimal. After an LLM is safety-aligned, its weights are
 156 biased toward safety objectives, weakening initialization for downstream task learning compared to
 157 the base model. As a result, finetuning a safety-aligned model solely on user data yields limited
 158 task performance and degraded safety-alignment. In contrast, we observe that **directly finetuning**
 159 **the base model on both user data and safety-alignment data is more effective**. This strategy
 160 leverages the well-known fact that base models provide strong initialization for downstream tasks.

161 To validate this claim, we evaluate the transferability of safety-aligned models and base model by
 162 comparing two finetuning strategies via Harmful Score (HS) and Finetuning Accuracy (FA) after

162
163
164 Table 1: Performance comparison of various safety-aligned LLMs and base model finetuning under
varying ratios p of harmful prompts in user data. SA denotes safety-alignment and FT denotes
finetuning. Numbers in (\cdot) indicate the amount of data used for safety-alignment or finetuning.

Methods	Harmful Score (\downarrow)				Finetune Accuracy (\uparrow)			
	$p = 0$	$p = 0.1$	$p = 0.3$	$p = 0.5$	$p = 0$	$p = 0.1$	$p = 0.3$	$p = 0.5$
SA (1,000) \rightarrow FT (1,000)	4.9	48.1	78.2	79.8	42.8	43.4	40.2	42.7
SA (5,000) \rightarrow FT (1,000)	3.3	22.8	61.7	71.1	41.3	41.9	39.4	39.7
SA (10,000) \rightarrow FT (1,000)	2.2	16.2	57.3	71.3	41.1	39.9	39.1	37.1
Repnose (Rosati et al. (2024))	2.7	29.9	67.0	75.7	37.4	37.0	36.3	36.0
Vaccine (Huang et al. (2024d))	1.3	5.4	35.0	57.5	22.9	23.2	21.7	20.3
Booster (Huang et al. (2024c))	2.3	5.9	65.1	75.0	44.5	44.0	44.4	43.5
Base \rightarrow SA (1,000) + FT (1,000)	0.9	2.0	4.3	15.7	47.6	47.9	45.6	45.0

174
175
176
177 Table 2: Gradient conflicts in two finetuning frameworks, measured by the cosine similarity between
gradients from each objective during 300 finetuning steps. SA denotes safety alignment and FT
denotes finetuning. Numbers in (\cdot) indicate data size. $Freq$ represents the frequency of conflicts,
while Avg represents average cosine similarity. p denotes the ratio of harmful prompts in user data.

Methods	$p = 0$		$p = 0.1$		$p = 0.3$		$p = 0.5$	
	Freq (%)	Avg	Freq (%)	Avg	Freq (%)	Avg	Freq (%)	Avg
SA (1,000) \rightarrow FT (1,000)	3.37	0.574	3.54	0.551	3.54	0.531	3.45	0.525
SA (5,000) \rightarrow FT (1,000)	4.27	0.540	3.86	0.525	4.71	0.500	4.30	0.487
SA (10,000) \rightarrow FT (1,000)	3.29	0.549	3.93	0.524	4.03	0.501	4.13	0.525
Base \rightarrow SA (1,000) + FT (1,000)	35.09	0.110	36.80	0.099	40.80	0.073	46.03	0.039

185
186 finetuning (see Section 6 for metric details): (i) finetuning safety-aligned models solely on user
187 data, and (ii) directly finetuning the base model on both user data and safety-alignment data. As
188 shown in Table 1, stronger safety-aligned models preserve safety more effectively but exhibit weaker
189 downstream task performance. In contrast, directly finetuning the base model achieves both robust
190 safety-alignment and strong downstream task performance. In this strategy, safety-alignment data
191 compensates the safety degradation caused by harmful finetuning attacks, while the base model’s
192 strong initialization supports effective downstream task learning. Remarkably, even this simple
193 strategy achieves performance comparable to existing baselines in both safety and downstream task.

194 **Limitations.** However, directly finetuning the base model on both user data and safety-alignment
195 data introduces **gradient conflicts**, as the model must simultaneously optimize two distinct objec-
196 tives. Gradient conflict is defined as opposing update directions between gradients from different
197 objectives, typically indicated by negative cosine similarity (Yu et al. (2020); Chen et al. (2020)).
198 To quantify these conflicts, we measure cosine similarities between gradients from user data and
199 safety-alignment data for each parameter, and record the cumulative frequency of negative simi-
200 larities along with the average cosine similarity over 300 training steps (see Appendix A.3 for this
201 choice). As shown in Table 2, when a safety-aligned model is finetuned only on user data, fewer
202 than 5% of gradients conflict during training. In contrast, when the base model is finetuned on both
203 user and safety-alignment data, more than 35% of gradients conflict, and the presence of harmful
204 prompts in user data further exacerbates this issue. These gradient conflicts destabilize training.

205 Motivated by this observation, we propose a **Refusal-Teacher (Ref-Teacher)-based finetuning**
206 **framework**, which alleviates gradient conflicts through alignment distillation and data filtering,
207 thereby stabilizing training and enhancing robustness against harmful finetuning attacks.

208 5 METHOD: REFUSAL-TEACHER-GUIDED FINETUNING FRAMEWORK

211 We propose the **Refusal-Teacher (Ref-Teacher)-guided finetuning framework**, which directly
212 finetunes the base model on both safety-alignment data and user data under the guidance of a Ref-
213 Teacher via **alignment distillation** and **data filtering**. Unlike prior works that adopts the alignment
214 stage, our approach introduces a **teacher preparation stage** to train the Ref-Teacher, followed by a
215 finetuning stage where the unaligned base model is trained with Ref-Teacher guidance. An overview
of our finetuning framework and a comparison with prior works are illustrated in Fig. 1.

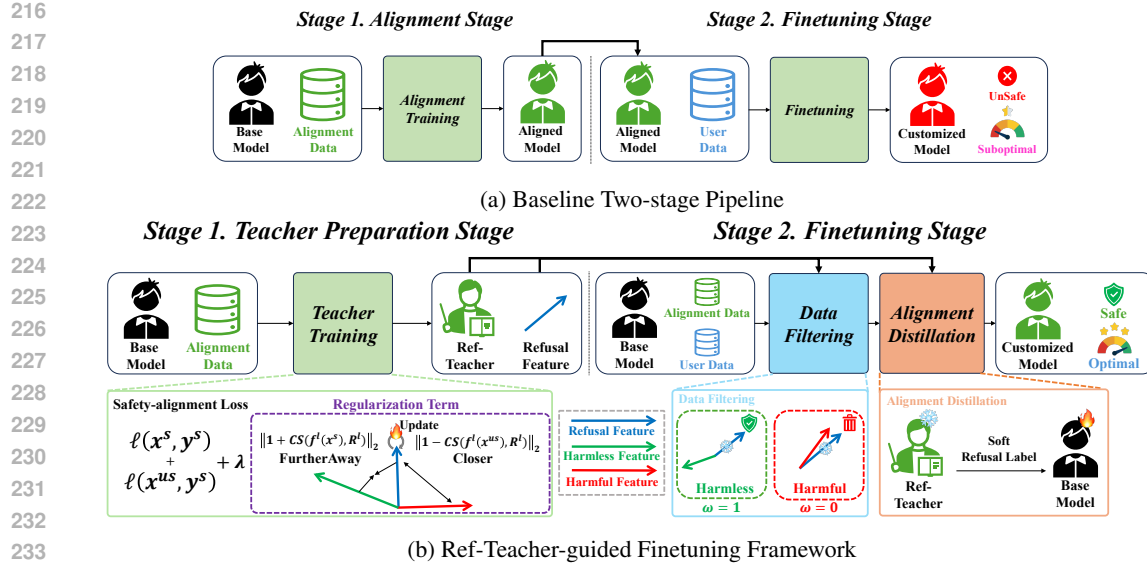


Figure 1: Overview comparison of finetuning frameworks. (a) The base model is first trained on safety-alignment data and then finetuned on user data, which often results in safety degradation and limited downstream task performance. (b) Ref-Teacher is trained on safety-alignment data utilizing refusal feature, and then the base model is directly finetuned on both user data and safety-alignment data under the guidance of Ref-Teacher via data filtering and alignment distillation.

5.1 TEACHER PREPARATION STAGE

The goal of the teacher preparation stage is to train a safety-aligned teacher model for alignment distillation and data filtering during finetuning stage. To this end, we leverage the **refusal feature** during safety-alignment to train the model to accurately distinguish harmful from harmless prompts.

The refusal feature (Arditi et al. (2024)) is a one-dimensional representation that encodes safety behavior, namely refusing harmful prompts while generating helpful responses for harmless ones. Formally, it is defined as the mean difference between feature representations of harmful and harmless prompts at a specific layer l of the LLM. Let x^s and x^{us} denote safe and unsafe prompts, respectively, and let $f^l(\cdot)$ denote the features of the last input token extracted from layer l . The refusal feature R^l is computed as $R^l = \frac{1}{N_{us}} \sum_{i=1}^{N_{us}} f^l(x_i^{us}) - \frac{1}{N_s} \sum_{i=1}^{N_s} f^l(x_i^s)$ where N_{us} and N_s denote the number of unsafe and safe prompts, respectively. Consequently, the refusal feature exhibit high cosine similarity with harmful prompt features and low similarity with harmless prompt features, enabling harmful and harmless prompts classification via a cosine similarity threshold.

Leveraging this property, we develop the **Ref-Teacher**, a safety-aligned LLM that (i) generates soft refusal labels for alignment distillation and (ii) more effectively distinguishes harmful from harmless prompts using its refusal feature for data filtering. To achieve two objectives, we train the model with a safety-alignment loss, a supervised loss on safety-alignment data where harmful prompts are paired with refusal responses and harmless prompts with helpful outputs. This loss encourages the model to refuse harmful requests while producing appropriate responses to harmless ones, thereby enforcing distinct behaviors across different prompt types.

To further enhance discrimination, we introduce a **regularization term** that enforces clearer separation between harmful and harmless prompt features based on the refusal feature. Specifically, this term encourages the cosine similarity between a refusal feature and harmful prompt features to approach 1, while pushing the similarity with harmless prompt features toward -1. To prevent corruption of internal representations, we control its strength using a hyperparameter λ . The final objective for teacher preparation stage is consist of the safety-alignment loss and this regularization:

$$\mathcal{L}_{\text{teacher}} = \frac{1}{N} \sum_{i=1}^N \left[\ell(x_i^s, y_i^s) + \ell(x_i^{us}, y_i^r) + \lambda \{ \|1 + \text{CS}(f^l(x_i^s), R^l)\|_2 + \|1 - \text{CS}(f^l(x_i^{us}), R^l)\|_2 \} \right] \quad (1)$$

270 where $\ell(\cdot, \cdot)$ denotes the cross-
 271 entropy loss, $CS(\cdot, \cdot)$ represents co-
 272 sine similarity, y^s and y^r are the
 273 harmless and refusal responses, re-
 274 spectively, and N is the number of
 275 training samples. As a result, the Ref-
 276 Teacher can generate appropriate re-
 277 fusal responses for harmful prompts
 278 while reliably distinguishing harmful
 279 from harmless inputs using its refusal
 280 feature.

281 In addition, we assume a setting
 282 where a pre-aligned model is unavail-
 283 able, making it impossible to extract
 284 the refusal feature in advance. To ad-
 285 dress this, we dynamically update the
 286 refusal feature during training at fixed
 287 intervals (cycles) based on its defini-
 288 tion. For each training step, harmful
 289 and harmless prompts are accu-
 290 mulated into sets S_{us} and S_s , and
 291 the refusal feature is updated for ev-
 292 ery cycle. Before the first update, we
 293 set $\lambda = 0$ to disable regularization,
 294 as the refusal feature is not yet reli-
 295 able. This **dynamic update strategy**
 296 removes the need for a separate align-
 297 ment stage, enabling the model to com-
 298 pute refusal feature and learn dis-
 299 criminative representations within a single
 300 training process. The complete algo-
 301 rithm for the teacher preparation stage
 302 is provided in Alg. 1.

Algorithm 1 Training Process of the Ref-Teacher Model

Require: Unsafe data x^{us} , Safe data x^s , Cycle number C , LoRA weight W , Regularization strength λ , Learning rate η
Ensure: Trained LoRA weight W , Refusal Feature R^l

Initialize Unsafe prompt set $S_{us} \leftarrow \emptyset$
 Initialize Safe prompt set $S_s \leftarrow \emptyset$
 Initialize Refusal feature $R^l \leftarrow \text{None}$
 Initialize Counter $c \leftarrow 0$

while not converged **do**

- Sample B examples each of x^{us} and x^s
- Append x^{us} to S_{us}
- Append x^s to S_s
- $c \leftarrow c + B$
- if** $c \geq C$ **then**
- Update $R^l \leftarrow \frac{1}{|S_{us}|} \sum_{x \in S_{us}} f^l(x) - \frac{1}{|S_s|} \sum_{x \in S_s} f^l(x)$
- Reset Unsafe prompt set $S_{us} \leftarrow \emptyset$
- Reset Safe prompt set $S_s \leftarrow \emptyset$
- $c \leftarrow 0$
- end if**
- if** R^l is None **then**
- $\lambda \leftarrow 0$
- end if**
- Compute $\mathcal{L}_{teacher}$ from Eq. 1
- Update $W \leftarrow W - \eta \cdot \nabla \mathcal{L}_{teacher}$

end while

return W and R^l

5.2 FINETUNING STAGE

301 In the finetuning stage, the Ref-Teacher is frozen and serves as a teacher for two complementary
 302 purposes: (i) providing alignment distillation and (ii) filtering harmful prompts from user data. This
 303 approach enables the base model to effectively learn user-specific tasks while maintaining strong
 304 safety-alignment by mitigating gradient conflicts that arise during finetuning.

305 **Alignment Distillation.** Knowledge distillation is a widely used technique for mitigating gradient
 306 conflicts in multi-objective learning. Prior works (Hinton et al. (2015); Furlanello et al. (2018);
 307 Müller et al. (2019); Yuan et al. (2020)) show that soft labels from a teacher provide richer supervi-
 308 sion and yield smoother loss surfaces than hard labels. Following this principle, we adopt alignment
 309 distillation to guide the base model when learning both user-specific tasks and safety-alignment.
 310 Specifically, the Ref-Teacher generates soft refusal labels, and the base model is trained with (i) a
 311 supervised loss on user data and (ii) a KL-divergence loss on safety-alignment data to align its pre-
 312 dictions with the Ref-Teacher’s soft labels. This distillation stabilizes training by reducing gradient
 313 conflicts, resulting in safe and appropriate responses for both harmful and user-specific inputs.

314 To ensure the reliability of these soft refusal labels, we reuse the safety-alignment data from the
 315 teacher preparation stage. Since the Ref-Teacher has already been trained on this data, it can generate
 316 accurate refusal responses. Moreover, as shown in Table 1, only a small subset of this data is needed
 317 to be reused, removing the need for additional alignment data for finetuning stage.

318 **Data Filtering.** While alignment distillation mitigates gradient conflicts between safety and user-
 319 specific task objectives, it alone cannot prevent these conflicts from being exacerbated by harmful
 320 finetuning attacks. To address this, we adopt data filtering as a complementary solution. In our
 321 framework, the Ref-Teacher filters harmful prompts from user data by leveraging its refusal feature
 322 to distinguish harmful from harmless inputs. Specifically, harmful data are identified by measuring
 323 the cosine similarity between the refusal feature R^l and the feature $f^l(x_i)$ of each input prompt.
 If the similarity exceeds a predefined threshold τ , the prompt is classified as harmful, otherwise as

324 harmless. This filtering mechanism is formulated as a binary filtering indicator ω_i :
 325

$$\omega_i = \begin{cases} 0, & \text{if } CS(R^l, f^l(x_i)) > \tau \\ 1, & \text{otherwise} \end{cases}. \quad (2)$$

329 In Eq. 2, prompts classified as harmful are excluded from the supervised finetuning loss by setting
 330 $\omega_i = 0$, since misclassifying harmful prompts as harmless could exacerbate gradient conflicts and
 331 destabilize training. To improve recall in harmful prompt classification, we set the threshold relatively
 332 high, ensuring that the Ref-Teacher is less likely to misclassify harmful prompts as harmless
 333 (even at the cost of discarding some harmless ones). Consequently, all data predicted to be harmful
 334 are discarded, ensuring finetuning is performed only on harmless prompts. This strategy preserves
 335 safety and stabilizes training by preventing even small amounts of harmful data.

336 **Overall Objective.** Our Ref-Teacher-guided finetuning strategy incorporates the dual-teacher mechanism,
 337 combining supervised finetuning on user data with alignment distillation on safety-alignment data.
 338 The overall loss function for finetuning stage is defined as:

$$\mathcal{L}_{ft} = \frac{1}{N_{user}} \sum_{i=1}^{N_{user}} \omega_i * \ell(x_i, y_i) + \alpha T^2 * \frac{1}{N_{align}} \sum_{i=1}^{N_{align}} \text{KL}(p_{t,i}^T || p_{s,i}^T), \quad (3)$$

343 where $\ell(x_i, y_i)$ is the cross-entropy loss on user data (x_i, y_i) weighted by ω_i . The second term is the
 344 alignment distillation loss on safety-alignment data, where KL denotes KL-divergence between the
 345 teacher (Ref-Teacher) distribution $p_{t,i}^T$ and the student (base model) distribution $p_{s,i}^T$ at temperature
 346 T . The softened distribution is $p_i^T = \frac{\exp(z_i/T)}{\sum_{j=1}^V \exp(z_j/T)}$ where z denotes the model logits and V is the
 347 vocabulary size. The hyperparameter α controls the relative weight of the distillation term.
 348

350 6 EXPERIMENT

352 We evaluate the effectiveness of our finetuning framework on safety-alignment and user-specific
 353 task performance under various settings. We varied the ratio of harmful prompts, the size of user
 354 data, the type of harmless prompts (GSM8K (Cobbe et al. (2021)), SST2 (Socher et al. (2013)),
 355 AGNEWS (Zhang et al. (2015)), AlpacaEval (Li et al. (2023))), and the base model (Llama3-8B
 356 (Llama Team (2024)), Gemma2-9B (Team et al. (2024)), Qwen2-7B (Team (2024))). Unless noted
 357 otherwise, we used Llama3-8B, 0.1 poison ratio, 1,000 user data, and GSM8K as harmless data.

358 **Datasets.** For teacher preparation stage, we used $N = 5,000$ harmful prompts with refusal
 359 responses from BeaverTails (Ji et al. (2023)), and $N = 5,000$ harmless prompts with helpful responses
 360 from Alpaca (Taori et al. (2023)). For finetuning stage, user data was constructed by mixing harmful
 361 and harmless samples with a specific poison ratio. The alignment data size N_{align} was set equal to
 362 the user data size N_{user} . All harmful prompts in experiments were sourced from BeaverTails, but
 363 distinct subsets were used for the teacher preparation, finetuning, and evaluation to avoid overlap.

364 **Metrics.** We evaluate both safety-alignment and task performance using two metrics: Harmful
 365 Score (HS) and Finetuning Accuracy (FA), following prior works (Huang et al. (2024a;b;c;d; 2025);
 366 Liu et al. (2025)). HS is the proportion of harmful responses among 1,000 outputs generated from
 367 BeaverTails test set, classified by the pretrained moderation model Beaver-Dam-7B (Ji et al. (2023)).
 368 FA is measured by downstream benchmarks for GSM8K, SST2, AGNEWS, and AlpacaEval, using
 369 1,000, 872, 1,000, and 122 samples, respectively. AlpacaEval was assessed by GPT-4o (Hurst et al.
 370 (2024)), following standard practices. Both HS and FA were evaluated after finetuning stage.

371 **Baselines.** We compare our framework against both alignment and finetuning-stage solutions. **SFT**
 372 is the standard supervised learning, aligning on harmful prompt-refusal pairs and then finetuning on
 373 user data. Among alignment-stage methods, **RepNoise** (Rosati et al. (2024)) removes harmful
 374 representations, **Vaccine** (Huang et al. (2024d)) enforces embedding invariance via perturbations, and
 375 **Booster** (Huang et al. (2024c)) simulates harmful finetuning to regularize harmful loss. All are fol-
 376 lowed by finetuning the aligned model on user data. For finetuning-stage solutions, applied to SFT-
 377 aligned models, **LDIFS** (Mukhoti et al. (2023)) constrains concept forgetting, while **Lisa** (Huang
 et al. (2024b)) alternates optimization between alignment and user data with a regularization term.

378
 379
 380
 Table 3: Performance under varying harmful prompts ratios p in user data. Lower harmful scores
 (↓) and higher finetuning accuracy (↑) indicate better performance. Results are averaged over seeds
 30, 42, and 50. Finetuning accuracy is not reported for $p = 1.0$ since harmless data is unavailable.

Methods	Harmful Score (↓)					Finetune Accuracy (↑)				
	$p = 0$	$p = 0.1$	$p = 0.3$	$p = 0.5$	$p = 1.0$	$p = 0$	$p = 0.1$	$p = 0.3$	$p = 0.5$	$p = 1.0$
SFT	2.2 \pm 0.1	16.2 \pm 0.4	57.3 \pm 0.6	71.3 \pm 0.6	76.7 \pm 0.4	41.1 \pm 0.0	39.9 \pm 0.6	39.1 \pm 0.2	37.1 \pm 0.6	-
Repnose (Rosati et al. (2024))	2.7 \pm 0.4	29.9 \pm 0.6	67.0 \pm 0.5	75.7 \pm 3.1	79.7 \pm 0.6	37.4 \pm 0.3	37.0 \pm 1.2	36.3 \pm 0.7	36.0 \pm 1.4	-
Vaccine (Huang et al. (2024d))	1.3 \pm 0.2	5.4 \pm 0.7	35.0 \pm 0.3	57.5 \pm 0.4	81.3 \pm 0.1	22.9 \pm 0.5	23.2 \pm 1.0	21.7 \pm 0.3	20.3 \pm 0.4	-
Booster (Huang et al. (2024c))	2.3 \pm 0.1	5.9 \pm 0.2	65.1 \pm 0.3	75.0 \pm 0.6	79.0 \pm 0.4	44.5 \pm 0.5	44.0 \pm 0.9	44.4 \pm 0.6	43.5 \pm 0.6	-
LDIFS (Mukhoti et al. (2023))	1.0 \pm 0.2	4.1 \pm 0.7	7.1 \pm 0.2	14.7 \pm 0.3	24.0 \pm 0.4	18.0 \pm 0.9	16.7 \pm 0.8	15.5 \pm 0.1	15.4 \pm 0.6	-
Lisa (Huang et al. (2024b))	1.4 \pm 0.2	5.3 \pm 0.1	25.9 \pm 1.5	49.2 \pm 0.7	67.3 \pm 1.0	38.3 \pm 0.7	38.9 \pm 0.9	37.8 \pm 0.9	36.2 \pm 0.5	-
Ref-Teacher (Ours)	0.9\pm0.3	1.0\pm0.5	0.6\pm0.1	0.9\pm0.3	1.3\pm0.2	48.8\pm0.5	49.0\pm0.5	45.5\pm0.9	44.8\pm0.5	-

388
 389
 Table 4: Performance comparison across varying amounts of user data. n denotes the user data size.

Methods	Harmful Score (↓)					Finetune Accuracy (↑)				
	n=1000	n=1500	n=2000	n=2500	Average	n=1000	n=1500	n=2000	n=2500	Average
SFT	16.7	39.4	55.8	63.9	44.0	40.6	42.9	44.5	45.3	43.3
Repnose (Rosati et al. (2024))	30.4	50.4	61.7	72.9	53.9	38.4	40.5	43.6	43.5	41.5
Vaccine (Huang et al. (2024d))	4.8	19.8	34.1	45.0	25.9	24.4	28.5	31.3	33.9	29.5
Booster (Huang et al. (2024c))	5.9	19.4	48.2	62.6	34.0	43.4	45.3	48.4	48.5	46.4
LDIFS (Mukhoti et al. (2023))	4.0	5.7	4.7	6.0	5.1	17.0	16.7	17.7	18.4	17.5
Lisa (Huang et al. (2024b))	5.3	8.2	10.4	12.8	9.2	38.3	37.8	40.3	42.7	39.8
Ref-Teacher (Ours)	0.5	0.9	0.9	1.0	0.8	49.0	50.1	52.1	51.8	50.8

400 6.1 EXPERIMENT RESULTS

401
 402
 403 **Robustness under Varying Harmful Prompt Ratio.** We evaluate our framework using HS and FA
 404 under varying ratios of harmful prompts p in user data, ranging from fully clean data ($p = 0$) to
 405 entirely harmful data ($p = 1.0$). Table 3 shows that our method consistently achieves the lowest HS
 406 and the highest FA across all values of p , outperforming all baselines. This effectiveness and robust-
 407 ness stems from directly finetuning the base model while mitigating gradient conflicts under harmful
 408 finetuning attacks through alignment distillation and data filtering with the Ref-Teacher. Moreover,
 409 alignment-stage baselines such as RepNoise (Rosati et al. (2024)), Vaccine (Huang et al. (2024d)),
 410 and Booster (Huang et al. (2024c)) degrade under high harmful ratios ($p \geq 0.3$), while finetuning-
 411 stage solutions such as LDIFS (Mukhoti et al. (2023)), Lisa (Huang et al. (2024b)), and our approach
 412 remain robust, maintaining lower HS. Among these, our Ref-Teacher-guided finetuning framework
 413 achieves the best performance in both safety-alignment and user-specific downstream tasks.

414 **Scalability with Varying Amounts of User Data.** We evaluate scalability of our framework by
 415 measuring HS and FA as the number of user data samples increases from 1,000 to 2,500. As shown
 416 in Table 4, our Ref-Teacher-guided finetuning strategy consistently achieves the best performance
 417 across all settings. For a fixed poison ratio, our method maintains low HS even as the absolute num-
 418 ber of harmful prompts grows with data size, demonstrating strong robustness in safety-alignment.
 419 At the same time, FA improves as more user data become available for user-specific tasks. These
 420 results validate the scalability and adaptability of our approach across varying data scales.

421 **Generalization across Diverse Finetuning Datasets.** In our default setting, GSM8K serves as the
 422 user-specific downstream task. To evaluate generalization across datasets, we replaced the harmless
 423 portion of user data with SST2, AGNEWS, and AlpacaEval samples, and measured HS and FA for
 424 our method and baselines. As shown in Table 5, our approach consistently yields the lowest HS and
 425 highest FA across all datasets. These results demonstrate the strong generalization of our framework,
 426 preserving both safety-alignment and task performance across diverse downstream tasks.

427 **Adaptability across Model Architectures.** We assess adaptability to diverse model architectures
 428 by training the Ref-Teacher on Gemma2-9B and Qwen2-7B, and finetuning each corresponding base
 429 model on safety-alignment and user data. To obtain the refusal feature, we select the optimal safety
 430 layer for harmfulness classification, which differs by architecture (Details are in Appendix B.1). Ta-
 431 ble 6 shows that our method consistently reduces harmfulness while improving user-specific down-
 432 stream performance across model architectures. These results demonstrate that our approach gen-
 433 eralizes across diverse LLM backbones rather than being restricted to a single architecture.

432 Table 5: Performance comparison across different downstream tasks.
433

434 Methods	435 GSM8K		436 SST2		437 AGNEWS		438 AlpacaEval		439 Average	
	440 HS ↓	441 FA ↑	442 HS ↓	443 FA ↑	444 HS ↓	445 FA ↑	446 HS ↓	447 FA ↑	448 HS ↓	449 FA ↑
SFT	16.7	40.6	33.5	93.4	28.2	82.8	23.7	32.7	20.4	49.9
Repoise (Rosati et al. (2024))	30.4	38.4	63.0	93.4	58.6	84.6	45.4	29.3	39.5	49.1
Vaccine (Huang et al. (2024d))	4.8	24.4	35.8	90.0	29.5	83.2	55.8	14.4	25.2	42.4
Booster (Huang et al. (2024c))	5.9	43.4	9.2	93.6	5.3	85.3	29.4	34.0	10.0	51.3
LDIFS (Mukhoti et al. (2023))	4.0	17.0	14.6	90.5	12.5	71.2	5.7	33.7	7.4	42.5
Lisa (Huang et al. (2024b))	5.3	38.3	21.4	93.4	14.9	84.5	10.1	29.6	10.3	49.2
Ref-Teacher (Ours)	0.5	49.0	1.3	94.5	1.2	86.1	2.4	34.6	1.1	52.8

440 Table 6: Performance comparison across different model architectures. Our Ref-Teacher-guided
441 finetuning strategy shows strong adaptability across Llama3-8B, Gemma2-9B, and Qwen2-7B.
442

443 Methods	444 Llama3-8B		445 Gemma2-9B		446 Qwen2-7B		447 Average	
	448 HS ↓	449 FA ↑	450 HS ↓	451 FA ↑	452 HS ↓	453 FA ↑	454 HS ↓	455 FA ↑
SFT	16.7	40.6	26.4	59.5	37.9	66.8	27.0	55.6
Repoise (Rosati et al. (2024))	30.4	38.4	26.2	57.1	25.4	63.7	27.3	53.1
Vaccine (Huang et al. (2024d))	4.8	24.4	18.0	52.5	10.2	63.6	11.0	46.8
Booster (Huang et al. (2024c))	5.9	43.4	2.3	58.4	4.9	70.0	4.4	57.3
LDIFS (Mukhoti et al. (2023))	4.0	17.0	3.1	36.0	10.7	64.1	5.9	39.0
Lisa (Huang et al. (2024b))	5.3	38.3	6.2	54.5	4.4	61.6	5.3	51.5
Ref-Teacher (Ours)	0.5	49.0	1.3	63.6	0.6	69.7	0.8	60.8

456 Table 7: Classification accuracy (%) during finetuning.
457458 Table 8: F1 Scores (%) of Ref-Teacher, guardrail models, and linear classifier across various jailbreaking attacks.
459

Datasets	Harmful	Harmless	Total
GSM8K	100.00	97.70	97.93
SST2	99.91	95.30	95.76
AGNEWS	99.91	99.86	99.87
AlpacaEval	99.90	77.04	79.33

Datasets	BeaverTails	JailbreakBench	Toxic-chat	GCG	AutoDAN-turbo
Linear Classifier	83.5	69.8	75.7	52.4	48.4
LLaMAGuard3-8B	64.1	88.7	57.0	89.7	9.3
OpenAI Moderation	67.8	74.7	44.4	81.0	52.2
Ref-Teacher ($\tau = 0$)	93.4	79.8	87.0	92.9	82.1

460 Table 9: Ablation study on safety
461 and task performance.
462

463 AD	464 Filtering	465 HS ↓		466 FA ↑	
		467 Freq (%)	468 Avg	469 Freq (%)	470 Avg
X	X	2.0	47.9		
O	X	2.2	46.2		
X	O	0.6	46.5		
O	O	0.5	49.0		

471 Table 10: Ablation study on gradient conflicts.
472

473 AD	474 Filtering	475 p = 0		476 p=0.1		477 p=0.3		478 p=0.5	
		479 Freq (%)	480 Avg	481 Freq (%)	482 Avg	483 Freq (%)	484 Avg	485 Freq (%)	486 Avg
X	X	35.09	0.110	36.80	0.099	40.80	0.073	46.03	0.039
O	X	32.26	0.131	34.02	0.117	37.78	0.090	42.55	0.055
X	O	36.11	0.102	36.51	0.097	37.80	0.087	39.91	0.073
O	O	30.02	0.140	29.60	0.143	28.93	0.145	28.29	0.149

487

6.2 ANALYSIS

Classification Performance of Ref-Teacher. We evaluate Ref-Teacher’s ability to classify harmful and harmless prompts during finetuning on GSM8K, SST2, AGNEWS, and AlpacaEval, achieving near-perfect accuracy on harmful prompts and consistently high accuracy on harmless ones (Table 7). For generalization, we test on JailbreakBench harmless prompts combined with harmful prompts from BeaverTails, JailbreakBench, Toxic-chat, GCG, and AutoDAN-turbo. Ref-Teacher, trained only on BeaverTails (harmful) and Alpaca (harmless), is compared against LLaMAGuard3-8B (LLaMA Team (2024)), OpenAI Moderation, and a linear classifier trained on LLaMA3-8B features using the same data. As shown in Table 8, the classifier performs well on in-distribution but degrades on unseen jailbreaks, whereas Ref-Teacher consistently outperforms all baselines, achieving high F1 scores even on advanced attacks (GCG, AutoDAN-turbo). These results demonstrate the accuracy and generalization of refusal-based classification for reliable harmful data filtering.

Ablation Study on Safety and Task Performance. We assess the impact of alignment distillation (AD) and data filtering (Filtering) on safety and task performance by removing each component. As shown in Table 9, AD alone improves neither safety nor finetuning accuracy, indicating that it cannot stabilize optimization when harmful prompts remain in user data. In contrast, Filtering alone reduces harmfulness but lowers finetuning accuracy due to reduced user data, which increases overfitting risk. These results highlight their complementary roles: AD stabilizes optimization but requires filtered data, whereas Filtering reduces harmfulness but risks overfitting without distillation. Their combination synergistically achieves strong task performance while preserving safety alignment.

486 Table 11: Computational Overhead across Baselines.
487

488 Methods	489 Alignment Stage		490 Finetuning Stage		491 Sum	
	492 GPUTime (s)	493 GPUMemory (GB)	494 GPUTime (s)	495 GPUMemory (GB)	496 GPUTime (s)	497 GPUMemory (GB)
SFT	0.91	7.84	1.59	9.31	2.50	17.15
Reprosne (Rosati et al. (2024))	4.27	15.27	1.59	9.31	5.86	24.58
Vaccine (Huang et al. (2024d))	1.79	7.84	1.59	9.31	3.38	17.15
Booster (Huang et al. (2024c))	3.92	9.39	1.59	9.31	5.51	18.70
LDIFS (Mukhoti et al. (2023))	0.91	7.84	1.95	16.51	2.86	24.35
Lisa (Huang et al. (2024b))	0.91	7.84	1.59	9.02	2.50	16.86
Ref-Teacher (Ours)	1.76	11.29	1.84	12.01	3.60	23.30

498 **Ablation Study on Gradient Conflicts.** We evaluate the contributions of alignment distillation
499 (AD) and data filtering (Filtering) on gradient conflicts by removing each component and varying
500 the harmful ratio p . Table 10 shows that AD alone reduces conflicted parameters on clean data
501 but loses effectiveness as p increases, while Filtering alone stabilizes the frequency of conflicts but
502 does not sufficiently mitigate it. Consequently, AD and Filtering complement each other in our
503 framework, mitigating gradient conflicts effectively under harmful finetuning attacks.

504 **Computational Overhead.** To quantify the computational overhead introduced by the Teacher
505 Preparation Stage, we measured both GPUTime and GPUMemory for the alignment stage and the
506 finetuning stage separately. All measurements were performed on four RTX 3090 GPUs, and Ta-
507 ble X reports the per-GPU GPUTime (average per-step runtime) and GPUMemory (average per-step
508 memory usage). As shown in Table 11, while Ref-Teacher does incur additional cost relative to SFT,
509 the increase is moderate compared to other baselines. Specifically, compared to SFT, Ref-Teacher
510 uses 44.0% more GPUTime and 35.9% more GPUMemory, yet achieves a 93.8% reduction in harm-
511 ful score and a 22.8% increase in finetuning accuracy. These results indicate that the computational
512 overhead is modest and well-justified given the substantial safety and utility improvements.

513 7 CONCLUSION

514 In this work, we address a key limitation of current two-stage Finetuning-as-a-Service (FaaS) prac-
515 tices, where providers first safety-align an LLM and then finetune the safety-aligned model on user
516 data. We observe that safety-aligned models offer weak initialization for downstream task learn-
517 ing, leading to suboptimal task performance and degraded safety when finetuning the safety-aligned
518 model on user data. To overcome this, we introduce the Refusal-Teacher (Ref-Teacher)-guided fine-
519 tuning framework, which directly finetunes the unaligned base model on both safety-alignment data
520 and user data under the guidance of a safety-aligned Ref-Teacher via alignment distillation and data
521 filtering. Extensive experiments demonstrate that our framework consistently achieves the lowest
522 harmful scores and the highest finetuning accuracy across diverse settings, outperforming baselines.
523 Overall, our approach offers a practical and effective solution for FaaS, ensuring strong user-specific
524 task performance while preserving safety-alignment against harmful finetuning attacks.

525 REFERENCES

526 Andy Ardit, Oscar Obeso, Aaquib Syed, Daniel Paleka, Nina Panickssery, Wes Gurnee, and
527 Neel Nanda. Refusal in language models is mediated by a single direction. *arXiv preprint*
528 *arXiv:2406.11717*, 2024.

529 Somnath Banerjee, Sayan Layek, Soham Tripathy, Sharu Kumar, Animesh Mukherjee, and Rima
530 Hazra. Safeinfer: Context adaptive decoding time safety alignment for large language models.
531 In *Proceedings of the AAAI Conference on Artificial Intelligence*, volume 39, pp. 27188–27196,
532 2025.

533 Jan Betley, Daniel Tan, Niels Warncke, Anna Szyber-Betley, Xuchan Bao, Martín Soto, Nathan
534 Labenz, and Owain Evans. Emergent misalignment: Narrow finetuning can produce broadly
535 misaligned llms. *arXiv preprint arXiv:2502.17424*, 2025.

536 Federico Bianchi, Mirac Suzgun, Giuseppe Attanasio, Paul Röttger, Dan Jurafsky, Tatsunori
537 Hashimoto, and James Zou. Safety-tuned llamas: Lessons from improving the safety of large
538 language models that follow instructions. *arXiv preprint arXiv:2309.07875*, 2023.

540 Patrick Chao, Alexander Robey, Edgar Dobriban, Hamed Hassani, George J Pappas, and Eric
 541 Wong. Jailbreaking black box large language models in twenty queries. *arXiv preprint*
 542 *arXiv:2310.08419*, 2023.

543 Patrick Chao, Edoardo Debenedetti, Alexander Robey, Maksym Andriushchenko, Francesco Croce,
 544 Vikash Sehwag, Edgar Dobriban, Nicolas Flammarion, George J. Pappas, Florian Tramèr, Hamed
 545 Hassani, and Eric Wong. Jailbreakbench: An open robustness benchmark for jailbreaking large
 546 language models, 2024.

547 Zhao Chen, Jiquan Ngiam, Yanping Huang, Thang Luong, Henrik Kretzschmar, Yuning Chai, and
 548 Dragomir Anguelov. Just pick a sign: Optimizing deep multitask models with gradient sign
 549 dropout. *Advances in Neural Information Processing Systems*, 33:2039–2050, 2020.

550 Karl Cobbe, Vineet Kosaraju, Mohammad Bavarian, Mark Chen, Heewoo Jun, Lukasz Kaiser,
 551 Matthias Plappert, Jerry Tworek, Jacob Hilton, Reiichiro Nakano, Christopher Hesse, and John
 552 Schulman. Training verifiers to solve math word problems. *arXiv preprint arXiv:2110.14168*,
 553 2021.

554 Yanrui Du, Sendong Zhao, Danyang Zhao, Ming Ma, Yuhang Chen, Liangyu Huo, Qing Yang,
 555 Dongliang Xu, and Bing Qin. Mogu: A framework for enhancing safety of open-sourced llms
 556 while preserving their usability. *arXiv preprint arXiv:2405.14488*, 2024.

557 Tommaso Furlanello, Zachary Lipton, Michael Tschannen, Laurent Itti, and Anima Anandkumar.
 558 Born again neural networks. In *International conference on machine learning*, pp. 1607–1616.
 559 PMLR, 2018.

560 Daya Guo, Dejian Yang, Haowei Zhang, Junxiao Song, Ruoyu Zhang, Runxin Xu, Qihao Zhu,
 561 Shirong Ma, Peiyi Wang, Xiao Bi, et al. Deepseek-r1: Incentivizing reasoning capability in llms
 562 via reinforcement learning. *arXiv preprint arXiv:2501.12948*, 2025.

563 Luxi He, Mengzhou Xia, and Peter Henderson. What is in your safe data? identifying benign data
 564 that breaks safety. *arXiv preprint arXiv:2404.01099*, 2024.

565 Geoffrey Hinton, Oriol Vinyals, and Jeff Dean. Distilling the knowledge in a neural network. *arXiv*
 566 *preprint arXiv:1503.02531*, 2015.

567 Lei Hsiung, Tianyu Pang, Yung-Chen Tang, Linyue Song, Tsung-Yi Ho, Pin-Yu Chen, and Yao-
 568 qing Yang. Why llm safety guardrails collapse after fine-tuning: A similarity analysis between
 569 alignment and fine-tuning datasets. *arXiv preprint arXiv:2506.05346*, 2025.

570 Chia-Yi Hsu, Yu-Lin Tsai, Chih-Hsun Lin, Pin-Yu Chen, Chia-Mu Yu, and Chun-Ying Huang. Safe
 571 lora: The silver lining of reducing safety risks when finetuning large language models. *Advances*
 572 *in Neural Information Processing Systems*, 37:65072–65094, 2024.

573 Edward J Hu, Yelong Shen, Phillip Wallis, Zeyuan Allen-Zhu, Yuanzhi Li, Shean Wang, Lu Wang,
 574 Weizhu Chen, et al. Lora: Low-rank adaptation of large language models. *ICLR*, 1(2):3, 2022.

575 Xiaomeng Hu, Pin-Yu Chen, and Tsung-Yi Ho. Gradient cuff: Detecting jailbreak attacks on large
 576 language models by exploring refusal loss landscapes. *arXiv preprint arXiv:2403.00867*, 2024.

577 Tiansheng Huang, Gautam Bhattacharya, Pratik Joshi, Josh Kimball, and Ling Liu. Antidote: Post-
 578 fine-tuning safety alignment for large language models against harmful fine-tuning. *arXiv preprint*
 579 *arXiv:2408.09600*, 2024a.

580 Tiansheng Huang, Sihao Hu, Fatih Ilhan, Selim Tekin, and Ling Liu. Lisa: Lazy safety alignment
 581 for large language models against harmful fine-tuning attack. *Advances in Neural Information*
 582 *Processing Systems*, 37:104521–104555, 2024b.

583 Tiansheng Huang, Sihao Hu, Fatih Ilhan, Selim Furkan Tekin, and Ling Liu. Booster: Tack-
 584 ling harmful fine-tuning for large language models via attenuating harmful perturbation. *arXiv*
 585 *preprint arXiv:2409.01586*, 2024c.

586 Tiansheng Huang, Sihao Hu, Fatih Ilhan, Selim Furkan Tekin, and Ling Liu. Vaccine: Perturbation-aware alignment for large lan-
 587 guage models against harmful fine-tuning attack. *arXiv preprint arXiv:2402.01109*, 2024d.

594 Tiansheng Huang, Sihao Hu, Fatih Ilhan, Selim Furkan Tekin, and Ling Liu. Virus: Harmful
 595 fine-tuning attack for large language models bypassing guardrail moderation. *arXiv preprint*
 596 *arXiv:2501.17433*, 2025.

597 Kuo-Han Hung, Ching-Yun Ko, Ambrish Rawat, I Chung, Winston H Hsu, Pin-Yu Chen, et al.
 598 Attention tracker: Detecting prompt injection attacks in llms. *arXiv preprint arXiv:2411.00348*,
 599 2024.

600 Aaron Hurst, Adam Lerer, Adam P Goucher, Adam Perelman, Aditya Ramesh, Aidan Clark, AJ Os-
 601 trow, Akila Welihinda, Alan Hayes, Alec Radford, et al. Gpt-4o system card. *arXiv preprint*
 602 *arXiv:2410.21276*, 2024.

603 Jiaming Ji, Mickel Liu, Josef Dai, Xuehai Pan, Chi Zhang, Ce Bian, Boyuan Chen, Ruiyang Sun,
 604 Yizhou Wang, and Yaodong Yang. Beavertails: Towards improved safety alignment of llm via
 605 a human-preference dataset. *Advances in Neural Information Processing Systems*, 36:24678–
 606 24704, 2023.

607 Albert Qiaochu Jiang, Alexandre Sablayrolles, Arthur Mensch, Chris Bamford, Devendra Singh
 608 Chaplot, Diego de Las Casas, Florian Bressand, Gianna Lengyel, Guillaume Lample, Lu-
 609 cile Saulnier, L'elio Renard Lavaud, Marie-Anne Lachaux, Pierre Stock, Teven Le Scao,
 610 Thibaut Lavril, Thomas Wang, Timothée Lacroix, and William El Sayed. Mistral 7b. *ArXiv*,
 611 *abs/2310.06825*, 2023. URL <https://api.semanticscholar.org/CorpusID:263830494>.

612 Simon Lermen, Charlie Rogers-Smith, and Jeffrey Ladish. Lora fine-tuning efficiently undoes safety
 613 training in llama 2-chat 70b. *arXiv preprint arXiv:2310.20624*, 2023.

614 Mingjie Li, Wai Man Si, Michael Backes, Yang Zhang, and Yisen Wang. Salora: Safety-alignment
 615 preserved low-rank adaptation. *arXiv preprint arXiv:2501.01765*, 2025.

616 Shen Li, Liuyi Yao, Lan Zhang, and Yaliang Li. Safety layers in aligned large language models:
 617 The key to llm security. *arXiv preprint arXiv:2408.17003*, 2024a.

618 Xiao Li, Zhuhong Li, Qiongxiao Li, Bingze Lee, Jinghao Cui, and Xiaolin Hu. Faster-gcg: Efficient
 619 discrete optimization jailbreak attacks against aligned large language models. *arXiv preprint*
 620 *arXiv:2410.15362*, 2024b.

621 Xuechen Li, Tianyi Zhang, Yann Dubois, Rohan Taori, Ishaan Gulrajani, Carlos Guestrin, Percy
 622 Liang, and Tatsunori B. Hashimoto. Alpacaeval: An automatic evaluator of instruction-following
 623 models. https://github.com/tatsu-lab/alpaca_eval, 5 2023.

624 Guozhi Liu, Weiwei Lin, Tiansheng Huang, Ruichao Mo, Qi Mu, and Li Shen. Targeted vaccine:
 625 Safety alignment for large language models against harmful fine-tuning via layer-wise perturba-
 626 tion. *arXiv preprint arXiv:2410.09760*, 2024.

627 Guozhi Liu, Qi Mu, Tiansheng Huang, Xinhua Wang, Li Shen, Weiwei Lin, and Zhang Li. Pharma-
 628 cist: Safety alignment data curation for large language models against harmful fine-tuning. *arXiv*
 629 *preprint arXiv:2510.10085*, 2025.

630 Xiaogeng Liu, Nan Xu, Muhan Chen, and Chaowei Xiao. Autodan: Generating stealthy jailbreak
 631 prompts on aligned large language models. *arXiv preprint arXiv:2310.04451*, 2023.

632 AI @ Meta Llama Team. The llama 3 herd of models, 2024. URL <https://arxiv.org/abs/2407.21783>.

633 Ilya Loshchilov and Frank Hutter. Decoupled weight decay regularization. *arXiv preprint*
 634 *arXiv:1711.05101*, 2017.

635 Jishnu Mukhoti, Yarin Gal, Philip HS Torr, and Puneet K Dokania. Fine-tuning can cripple your
 636 foundation model; preserving features may be the solution. *arXiv preprint arXiv:2308.13320*,
 637 2023.

638 Rafael Müller, Simon Kornblith, and Geoffrey E Hinton. When does label smoothing help? *Ad-*
 639 *vances in neural information processing systems*, 32, 2019.

648 Long Ouyang, Jeffrey Wu, Xu Jiang, Diogo Almeida, Carroll Wainwright, Pamela Mishkin, Chong
 649 Zhang, Sandhini Agarwal, Katarina Slama, Alex Ray, et al. Training language models to fol-
 650 low instructions with human feedback. *Advances in neural information processing systems*, 35:
 651 27730–27744, 2022.

652 Samuele Poppi, Zheng-Xin Yong, Yifei He, Bobbie Chern, Han Zhao, Aobo Yang, and Jianfeng
 653 Chi. Towards understanding the fragility of multilingual llms against fine-tuning attacks. *arXiv*
 654 *preprint arXiv:2410.18210*, 2024.

655 et al. Qi. Constrain-sft: A supervised fine-tuning approach to enhance safety alignment in large
 656 language models. *Proceedings of NeurIPS 2024*, 37:95174, 2024. URL <https://nips.cc/virtual/2024/poster/95174>.

657 Xiangyu Qi, Yi Zeng, Tinghao Xie, Pin-Yu Chen, Ruoxi Jia, Prateek Mittal, and Peter Henderson.
 658 Fine-tuning aligned language models compromises safety, even when users do not intend to!
 659 *arXiv preprint arXiv:2310.03693*, 2023.

660 Rafael Rafailov, Archit Sharma, Eric Mitchell, Christopher D Manning, Stefano Ermon, and Chelsea
 661 Finn. Direct preference optimization: Your language model is secretly a reward model. *Advances*
 662 *in Neural Information Processing Systems*, 36:53728–53741, 2023.

663 LG Research, Kyunghoon Bae, Eunbi Choi, Kibong Choi, Stanley Jungkyu Choi, Yemuk Choi,
 664 Seokhee Hong, Junwon Hwang, Hyojin Jeon, Kijeong Jeon, et al. Exaone deep: Reasoning
 665 enhanced language models. *arXiv preprint arXiv:2503.12524*, 2025.

666 Domenic Rosati, Jan Wehner, Kai Williams, Lukasz Bartoszcze, Robie Gonzales, Subhabrata Ma-
 667 jumdar, Hassan Sajjad, Frank Rudzicz, et al. Representation noising: A defence mechanism
 668 against harmful finetuning. *Advances in Neural Information Processing Systems*, 37:12636–
 669 12676, 2024.

670 Abhay Sheshadri, Aidan Ewart, Phillip Guo, Aengus Lynch, Cindy Wu, Vivek Hebbar, Henry
 671 Sleight, Asa Cooper Stickland, Ethan Perez, Dylan Hadfield-Menell, et al. Targeted latent ad-
 672 versarial training improves robustness to persistent harmful behaviors in llms. *arXiv e-prints*, pp.
 673 arXiv–2407, 2024a.

674 Abhay Sheshadri, Aidan Ewart, Phillip Guo, Aengus Lynch, Cindy Wu, Vivek Hebbar, Henry
 675 Sleight, Asa Cooper Stickland, Ethan Perez, Dylan Hadfield-Menell, et al. Latent ad-
 676 versarial training improves robustness to persistent harmful behaviors in llms. *arXiv preprint*
 677 *arXiv:2407.15549*, 2024b.

678 Richard Socher, Alex Perelygin, Jean Wu, Jason Chuang, Christopher D. Manning, Andrew Ng,
 679 and Christopher Potts. Recursive deep models for semantic compositionality over a sentiment
 680 treebank. In *Proceedings of the 2013 Conference on Empirical Methods in Natural Language
 681 Processing*, pp. 1631–1642, Seattle, Washington, USA, October 2013. Association for Compu-
 682 tational Linguistics. URL <https://www.aclweb.org/anthology/D13-1170>.

683 Rishabh Iyer, Bhrugu Bharathi, Long Phan, Andy Zhou, Alice Gatti, Tarun Suresh, Maxwell
 684 Lin, Justin Wang, Rowan Wang, Ron Arel, et al. Tamper-resistant safeguards for open-weight
 685 llms. *arXiv preprint arXiv:2408.00761*, 2024.

686 Rohan Taori, Ishaan Gulrajani, Tianyi Zhang, Yann Dubois, Xuechen Li, Carlos Guestrin, Percy
 687 Liang, and Tatsunori B. Hashimoto. Stanford alpaca: An instruction-following llama model.
 688 https://github.com/tatsu-lab/stanford_alpaca, 2023.

689 Gemma Team, Morgane Riviere, Shreya Pathak, Pier Giuseppe Sessa, Cassidy Hardin, Surya Bhu-
 690 patiraju, Léonard Hussenot, Thomas Mesnard, Bobak Shahriari, Alexandre Ramé, et al. Gemma
 691 2: Improving open language models at a practical size. *arXiv preprint arXiv:2408.00118*, 2024.

692 Qwen Team. Qwen2 technical report. *arXiv preprint arXiv:2407.10671*, 2, 2024.

693 Hugo Touvron, Thibaut Lavril, Gautier Izacard, Xavier Martinet, Marie-Anne Lachaux, Timothée
 694 Lacroix, Baptiste Rozière, Naman Goyal, Eric Hambro, Faisal Azhar, et al. Llama: Open and
 695 efficient foundation language models. *arXiv preprint arXiv:2302.13971*, 2023.

702 Xuguang Wang, Daoyuan Wu, Zhenlan Ji, Zongjie Li, Pingchuan Ma, Shuai Wang, Yingjiu Li,
 703 Yang Liu, Ning Liu, and Juergen Rahmel. Selfdefend: Llms can defend themselves against
 704 jailbreaking in a practical manner. *arXiv preprint arXiv:2406.05498*, 2024.

705 et al. Wei. Freeze: A method to preserve safety alignment during fine-tuning of large language
 706 models. *Proceedings of NeurIPS 2024*, 37:96357, 2024. URL <https://neurips.cc/virtual/2024/poster/96357>.

709 Sophie Xhonneux, Alessandro Sordoni, Stephan Günnemann, Gauthier Gidel, and Leo Schwinn.
 710 Efficient adversarial training in llms with continuous attacks. *arXiv preprint arXiv:2405.15589*,
 711 2024.

712 Yuxin Xiao, Sana Tonekaboni, Walter Gerych, Vinith Suriyakumar, and Marzyeh Ghassemi. When
 713 style breaks safety: Defending language models against superficial style alignment. *arXiv preprint
 714 arXiv:2506.07452*, 2025.

716 Yueqi Xie, Minghong Fang, Renjie Pi, and Neil Gong. Gradsafe: Detecting jailbreak prompts for
 717 llms via safety-critical gradient analysis. *arXiv preprint arXiv:2402.13494*, 2024.

718 Zhangchen Xu, Fengqing Jiang, Luyao Niu, Jinyuan Jia, Bill Yuchen Lin, and Radha Poovendran.
 719 Safedecoding: Defending against jailbreak attacks via safety-aware decoding. *arXiv preprint
 720 arXiv:2402.08983*, 2024.

722 Shuo Yang, Qihui Zhang, Yuyang Liu, Yue Huang, Xiaojun Jia, Kunpeng Ning, Jiayu Yao, Jigang
 723 Wang, Hailiang Dai, Yibing Song, et al. Asft: Anchoring safety during lilm fine-tuning within
 724 narrow safety basin. *arXiv preprint arXiv:2506.08473*, 2025.

725 Xin Yi, Shunfan Zheng, Linlin Wang, Gerard de Melo, Xiaoling Wang, and Liang He. Nlsr: Neuron-
 726 level safety realignment of large language models against harmful fine-tuning. In *Proceedings of
 727 the AAAI Conference on Artificial Intelligence*, volume 39, pp. 25706–25714, 2025.

729 Lei Yu, Virginie Do, Karen Hambardzumyan, and Nicola Cancedda. Robust lilm safeguarding via
 730 refusal feature adversarial training. *arXiv preprint arXiv:2409.20089*, 2024.

731 Tianhe Yu, Saurabh Kumar, Abhishek Gupta, Sergey Levine, Karol Hausman, and Chelsea Finn.
 732 Gradient surgery for multi-task learning. *Advances in neural information processing systems*, 33:
 733 5824–5836, 2020.

735 Li Yuan, Francis EH Tay, Guilin Li, Tao Wang, and Jiashi Feng. Revisiting knowledge distillation
 736 via label smoothing regularization. In *Proceedings of the IEEE/CVF conference on computer
 737 vision and pattern recognition*, pp. 3903–3911, 2020.

738 Qiusi Zhan, Richard Fang, Rohan Bindu, Akul Gupta, Tatsunori Hashimoto, and Daniel Kang.
 739 Removing rlhf protections in gpt-4 via fine-tuning. *arXiv preprint arXiv:2311.05553*, 2023.

740 Xiang Zhang, Junbo Jake Zhao, and Yann LeCun. Character-level convolutional networks for text
 741 classification. In *NIPS*, 2015.

743 Yuqi Zhang, Liang Ding, Lefei Zhang, and Dacheng Tao. Intention analysis makes llms a good
 744 jailbreak defender. *arXiv preprint arXiv:2401.06561*, 2024.

746 Zhengyue Zhao, Xiaoyun Zhang, Kaidi Xu, Xing Hu, Rui Zhang, Zidong Du, Qi Guo, and Yunji
 747 Chen. Adversarial contrastive decoding: Boosting safety alignment of large language models via
 748 opposite prompt optimization. *arXiv preprint arXiv:2406.16743*, 2024.

749 Andy Zou, Zifan Wang, J. Zico Kolter, and Matt Fredrikson. Universal and transferable adversarial
 750 attacks on aligned language models, 2023.

751 Andy Zou, Long Phan, Justin Wang, Derek Duenas, Maxwell Lin, Maksym Andriushchenko, J Zico
 752 Kolter, Matt Fredrikson, and Dan Hendrycks. Improving alignment and robustness with circuit
 753 breakers. In *The Thirty-eighth Annual Conference on Neural Information Processing Systems*,
 754 2024.

755

APPENDIX

A EXPERIMENT DETAILS

A.1 TRAINING SETUP

In the teacher preparation stage, we train the Refusal-Teacher (Ref-Teacher) model for 20 epochs using batches of size 10, consisting of 5 harmful and 5 harmless prompts, with a learning rate of $5e^{-4}$. During the finetuning stage, we train the base model with Ref-Teacher for 20 epochs using 20 batches (10 harmful data and 10 harmless data), with a learning rate of $1e^{-5}$. For the AlpacaEval dataset (Li et al. (2023)), due to its small size, we train the base model for 100 epochs using 700 prompts. In both stages, we apply LoRA (Hu et al. (2022)) with a rank of 32, targeting the query, key, and value components of the attention modules. Also, we use the AdamW optimizer (Loshchilov & Hutter (2017)) with a weight decay of 0.1 and a constant learning rate schedule. All experiments are conducted on four RTX3090 GPUs.

A.2 HYPERPARAMETERS FOR OUR METHOD

Our proposed framework introduces several additional hyperparameters. First, in teacher preparation stage, we set the regularization strength for training Ref-Teacher model to $\lambda = 0.1$. Refusal features are extracted from specific layer in LLMs: $l = 12$ for LLAMA3-8B, $l = 11$ for Gemma2-9B, $l = 18$ for Qwen2-7B. The refusal features are updated periodically every $C = 6$ cycles, with each update performed using 30 harmful and 30 harmless prompts. During finetuning stage, for harmful and harmless classification using the Ref-Teacher model, we use a threshold of 0.9 to maximize the recall of harmful prompts. For alignment distillation, we set the distillation strength $\alpha = 0.1$ and use a the temperature $T = 1$. Ablation studies to identify the optimal values for these hyperparameters are presented in Sec. B. All the other hyperparameters for the baseline methods follow the settings specified in their respective original papers (Mukhoti et al. (2023); Huang et al. (2024c;d;b); Rosati et al. (2024)).

A.3 MEASURING GRADIENT CONFLICTS

We showed that directly finetuning the base model on both user data and safety-alignment data introduces gradient conflicts, which we measured using negative cosine similarities between gradients from the two datasets. Specifically, we reported the average frequency of negative cosine similarities and the average cosine similarity values accumulated over the first 300 training steps. We focus on this range because, after 300 steps, even when training on the same dataset, the signal-to-noise ratio (SNR) decreases sharply, making noise more dominant and causing negative cosine similarities to occur more frequently. Figure A2 reports the measured SNR when finetuning a safety-aligned model on user data, showing that SNR drops to very low values beyond 300 steps. Although gradients from the same dataset are theoretically expected to exhibit very few negative cosine similarities, we observed that their frequency increases after 300 steps under this finetuning setup. For this reason, we present negative cosine similarity statistics only up to 300 steps, as shown in Tables 2 and 10.

B EXPERIMENTS FOR FINDING OPTIMAL HYPERPARAMETERS

B.1 LAYER SELECTION FOR REFUSAL FEATURE EXTRACTION

The refusal feature reflects the model’s ability to distinguish between harmful and harmless prompts and to generate refusal responses only for harmful inputs. Therefore, it is most effective to extract the refusal feature from a layer that maximizes the distinction between harmful and harmless prompt representations. Based on a prior work (Li et al. (2024a)) suggesting that such layers are typically located in the middle layers of LLMs, we identify the optimal layer by evaluating classification accuracy and the norm difference between the average features of harmful and harmless prompts across 8 different layers. As shown in Table A1, both the classification accuracy and norm differences vary across layers. For each layer, the classification threshold is optimized to maximize classification performance. As a result, we used $l = 11$ for the Gemma2-9B (Team et al. (2024)) and $l = 18$

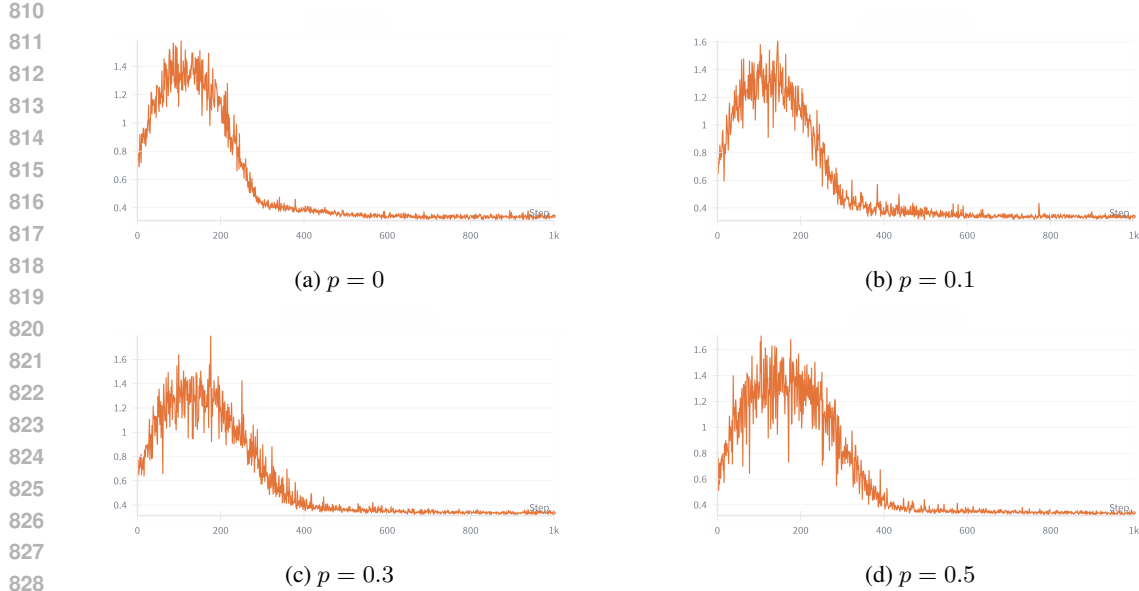


Figure A2: Signal-to-noise ratio (SNR) measured when finetuning a safety-aligned model solely on user data. SNR values consistently drop after 300 training steps across varying harmful ratios p , making noise dominant and increasing the frequency of negative cosine similarities between gradients.

Table A1: Classification accuracy and feature L1-norm differences across layers for identifying the optimal layer index used to extract refusal features in Gemma2-9B-it and Qwen2-7B-Instruct. The selected layer used in our experiments is highlighted in bold. For each layer, features are extracted from the last input token, and classification thresholds are optimized.

(a) Gemma2-9B-it							
Layer idx	Threshold	Harmful Acc (%)	Harmless Acc (%)	Acc (%)	Harmful Avg	Harmless Avg	Diff
7	0.0055	76.6	93.4	85.0	0.0239	-0.0090	0.0329
8	0.0225	69.8	93.8	81.8	0.0374	0.0080	0.0294
9	0.0510	89.6	96.6	93.1	0.0878	0.0303	0.0575
10	0.0530	93.8	95.0	94.4	0.0949	0.0363	0.0586
11	0.0245	96.2	98.6	97.4	0.0844	-0.0020	0.0864
12	0.0555	91.4	96.4	93.9	0.1133	0.0319	0.0814
13	0.0570	90.8	92.8	91.8	0.1285	0.0346	0.0939
14	0.184	86.6	91.2	88.9	0.2629	0.1524	0.0111

(b) Qwen2-7B-Instruct							
Layer idx	Threshold	Harmful Acc (%)	Harmless Acc (%)	Acc (%)	Harmful Avg	Harmless Avg	Diff
13	0.046	96.4	98.6	97.5	0.1814	0.0153	0.1661
14	0.118	97.2	97.8	97.5	0.2622	0.0875	0.1747
15	0.060	98.0	98.2	98.1	0.2297	0.0265	0.2032
16	0.145	96.2	99.2	97.7	0.3003	0.1093	0.1910
17	0.164	98.6	97.8	98.2	0.3709	0.1326	0.2383
18	0.195	98.6	99.8	99.2	0.4166	0.1551	0.2615
19	0.163	97.4	99.6	98.5	0.3555	0.1262	0.2293
20	0.055	95.0	99.4	97.2	0.2458	0.0211	0.2247

for the Qwen2-7B (Team (2024) in all of our experiments. For Llama3-8B, we adopted $l = 12$, following a prior work (Arditi et al. (2024)). Additionally, we used the feature corresponding to the last input token, as it encodes the entire sentence due to the language model’s causal structure and attention masking.

864
865 Table A2: Effect of cycle (C) on
866 the Ref-Teacher performance.
867

Cycle	$N_{us} = N_s$	HS (↓)	FA (↑)
6	30	0.5	49.0
20	100	1.1	47.8
100	500	1.1	47.7
200	1000	1.2	46.8

868
869 Table A3: Varying λ .
870
871

λ	HS (↓)	FA (↑)
0.05	0.7	48.4
0.1	0.5	49.0
0.3	1.0	48.3
0.5	1.0	48.3
1.0	1.6	47.7

872
873 Table A4: Varying Threshold.
874
875

Threshold	HS (↓)	FA (↑)
0	0.9	47.8
0.3	0.6	46.2
0.5	1.4	47.2
0.7	1.0	47.1
0.9	0.5	49.0

876
877 B.2 EFFECT OF CYCLE LENGTH ON REFUSAL FEATURE UPDATES
878
879

880 During the teacher preparation stage, the cycle determines both the interval and the number of samples used to update the refusal feature, which serves as important reference for distinguishing between features of harmful and harmless prompts in our Ref-Teacher model. A short cycle updates the refusal feature more frequently but with fewer samples, which can lead to unstable training due to variance of refusal features. In contrast, a long cycle uses more samples for each update but, due to its infrequent updates, may overfit to suboptimal refusal feature. Table A2 presents the harmful score (HS) and finetuning accuracy (FA) across different cycle lengths and the corresponding number of samples used for updating the standard refusal feature. The results show that frequent updates with a short cycle help the Ref-Teacher model more effectively separate harmful from harmless prompts and generate appropriate refusal responses to harmful inputs.

881
882 B.3 EFFECT OF REGULARIZATION STRENGTH (λ) ON REF-TEACHER MODEL TRAINING
883
884

885 The λ value in Eq. 1 of main manuscript controls the strength of the regularization term that encourages distinct separation between the features of harmful and harmless prompts in the Ref-Teacher model during the teacher preparation stage. An overly strong regularization term may disrupt the internal representations of the Ref-Teacher model, while a weak regularization term may reduce the Ref-Teacher model’s ability to distinguish between harmful and harmless prompts based on its refusal feature. Therefore, selecting an appropriate λ value is critical for effective training of the Ref-Teacher model and subsequent finetuning. Table A3 presents the finetuning performance using Ref-Teacher models trained with different λ values. The results show that a λ value of 0.1 achieves the lowest harmful score (HS) and the highest finetuning accuracy (FA), indicating its effectiveness as an optimal hyperparameter choice.

886
887 B.4 EFFECT OF THRESHOLD VALUES ON FINETUNING
888

889 The threshold τ in Eq. 2 is a key hyperparameter used as a standard to classify harmful prompts by 900 measuring the similarity between input prompt features and the refusal feature in the Ref-Teacher 901 model during the finetuning stage. We predicted prompts with similarity above the threshold as 902 harmful, while those below the threshold are classified as harmless. Therefore, a threshold that is 903 too low may misclassify harmful prompts as harmless, thereby introducing safety risks by allowing 904 harmful prompts to be included in finetuning. Conversely, a threshold that is too high may 905 incorrectly filter out harmless prompts misclassified as harmful, leading to reduced finetuning accuracy. 906 As shown in Table A4, we evaluate the impact of varying threshold values. The results indicate 907 that a threshold of 0.9 yields the lowest harmful score and the highest finetuning accuracy. This 908 optimal performance is attributed to the near-perfect alignment of harmful prompt features with the 909 refusal feature, resulting in the similarity values close to 1, in the Ref-Teacher model, as illustrated 910 in Table 7 of the main manuscript.

911
912 B.5 EFFECT OF ALIGNMENT DISTILLATION HYPERPARAMETERS
913

914 Knowledge distillation typically involves two key hyperparameters: temperature T , which controls 915 the softness of the teacher predictions, and the distillation weight α , which balances the influence 916 of the distillation loss. To evaluate their impact, we measure both the harmful score and finetuning 917 accuracy across various values of T and α . As shown in Table A5, higher values of T lead to increased harmful scores, likely due to the student model not closely following the Ref-Teacher 918 model’s predictions. In contrast, higher values of α reduce the harmful score but also lower the fine-

918
919 Table A5: Impact of temperature (T) and distillation weight (α) on Harmful Score (HS) and Fine-
920 tuning Accuracy (FA). The best-performing setting ($T = 1.0, \alpha = 0.1$) is highlighted in bold.
921
922
923
924
925

Temperature T	α	HS (↓)	FA (↑)
1.0	0.1	0.5	49.0
1.0	0.3	1.3	45.3
1.0	0.5	1.2	47.9
1.0	1.0	1.2	44.6
1.0	5.0	0.9	40.5
2.0	0.1	0.9	45.6
2.0	0.3	0.7	44.2
2.0	0.5	1.0	43.4
2.0	1.0	0.5	42.8
2.0	5.0	0.6	26.1
5.0	0.1	12.8	46.7
5.0	0.3	3.4	46.5
5.0	0.5	3.1	45.2
5.0	1.0	2.2	44.2
5.0	5.0	2.4	33.7

934
935 Table A6: Impact of data filtering on baseline. *HS* denotes Harmful Score (lower is better), and *FA*
936 denotes Finetuning Accuracy (higher is better).
937
938
939
940
941
942
943
944

Methods	No Filtering		LLaMAGuard		Ref-Teacher	
	HS	FA	HS	FA	HS	FA
SFT	16.7	40.6	6.6	40.4	1.7	43.3
RepNoise (Rosati et al. (2024))	30.4	38.4	13.2	37.2	2.5	36.7
Vaccine (Huang et al. (2024d))	4.8	24.4	1.9	22.7	1.3	22.4
Booster (Huang et al. (2024c))	5.9	43.4	3.2	43.7	0.9	44.2
LDIFS (Mukhoti et al. (2023))	4.0	17.0	2.6	17.4	1.1	16.1
Lisa (Huang et al. (2024b))	5.3	38.3	2.0	37.6	1.3	38.5
Ref-Teacher (Ours)	2.2	46.2	0.5	49.0	0.5	49.0

945
946 tuning accuracy, as excessive emphasis on the alignment loss weakens user-specific downstream task
947 performance. Among these hyperparameter values, $T = 1$ and $\alpha = 0.1$ yield the best overall per-
948 formance. This setting allows the student model to closely follow the well-aligned refusal responses
949 of the Ref-Teacher model, while keeping the alignment loss moderate to preserve downstream task
950 performance.
951

952 C ADDITIONAL EXPERIMENTS

953 C.1 COMPARISON TO BASELINES WITH GUARDRAIL-BASED FILTERING.

954
955 Our proposed finetuning framework incorporates a data filtering process guided by the Ref-Teacher
956 model, which is a fundamental defense against harmful finetuning attacks but has not yet been ex-
957 plored in the Finetuning-as-a-Service (FaaS) setting. To ensure that the superiority of our frame-
958 work does not arise merely from data filtering, we additionally apply two filtering strategies,
959 LLaMAGuard3-8B Llama Team (2024) and Ref-Teacher, to all baseline methods. Specifically, each
960 baseline finetunes a safety-aligned model on user data filtered by (1) LLaMAGuard3-8B, which re-
961 moves 5.7% of prompts, or (2) our Ref-Teacher filter, which removes 12.2% of prompts when 100
962 harmful prompts are included among 1,000 user prompts. As shown in Table A6, both filtering
963 methods reduces harmful scores across all baselines. Nevertheless, our framework consistently out-
964 performs these improvements without relying on any external guardrail. This result is consistent
965 with Table A10, where data filtering with Ref-Teacher achieves comparable safety gains but still
966 falls short of the full effectiveness of our method.
967

968 C.2 GENERALIZATION UNDER CROSS-DATASET FINETUNING

969 We conduct a cross-dataset evaluation to further assess generalization in the finetuning stage. Specif-
970 ically, both the Ref-Teacher model and the safety-aligned models are trained on BeaverTails (Ji

972 Table A7: Cross-Dataset Evaluation (BeaverTails (Ji et al. (2023)) → JailbreakBench (Chao et al.
 973 (2024))). *HS* denotes Harmful Score (lower is better), and *FA* denotes Finetuning Accuracy (higher
 974 is better).

976 Aligned Model	977 HS (In-Domain) ↓	978 FA (In-Domain) ↑	979 HS (Out-Domain) ↓	980 FA (Out-Domain) ↑
SFT	16.7	40.6	93.0	40.6
RepNoise (Rosati et al. (2024))	30.4	38.4	90.0	35.7
Vaccine (Huang et al. (2024d))	4.8	24.4	15.0	23.6
Booster (Huang et al. (2024c))	5.9	43.4	4.0	43.4
LDIFS (Mukhoti et al. (2023))	4.0	17.0	81.0	17.0
Lisa (Huang et al. (2024b))	5.3	38.3	9.0	35.7
Ref-Teacher (Ours)	0.5	49.0	2.0	46.6

983 Table A8: Performance on Llama3-8B-Instruct (Llama Team (2024)) under the pre-aligned LLM
 984 setting. Ref-Teacher* uses the raw instruct model as the Ref-Teacher without additional training,
 985 while Ref-Teacher denotes the model trained under our framework.

987 Method	988 HS (↓)	989 FA (↑)
SFT	64.0	66.0
LDIFS (Mukhoti et al. (2023))	15.9	66.8
SafeInstruct (Bianchi et al. (2023))	26.9	66.4
Lisa (Huang et al. (2024b))	28.1	60.6
Antidote (Huang et al. (2024a))	17.4	59.3
Ref-Teacher*	13.9	65.8
Ref-Teacher	5.4	66.5

995 et al. (2023)), and finetuning is then performed on JailbreakBench (Chao et al. (2024)). As shown
 996 in Table A7, several baselines suffer substantial performance degradation under this harmful data
 997 distribution shift, particularly in terms of harmfulness. In contrast, our Ref-Teacher-guided frame-
 998 work consistently achieves the lowest harmful scores and the highest finetuning accuracy in both
 999 in-domain and out-of-domain settings, demonstrating strong generalization across datasets.

1001 C.3 DISCUSSION OF THE PRE-ALIGNED LLM SETTING AND REF-TEACHER ADAPTATION

1003 In practice, many safety-aligned LLMs are already available, such as Llama3-8B-
 1004 Instruct Llama Team (2024), Gemma2-9B-it Team et al. (2024), and Qwen2-7B-Instruct Team
 1005 (2024). However, following prior studies Huang et al. (2024b;d;a;c), we assume that such
 1006 pre-aligned models are unavailable and begin from a base LLM. This assumption ensures a fair
 1007 comparison with alignment-stage methods.

1008 This setting is also realistic for new FaaS providers that have not yet established a safety-aligned
 1009 model. These organizations must decide how to construct one that remains robust against harmful
 1010 finetuning. They can either (1) adopt an alignment-stage approach or (2) perform standard su-
 1011 pervised safety-alignment followed by a finetuning-stage defense. In this context, our framework
 1012 introduces a specialized safety-aligned model that reliably identifies harmful prompts and provides
 1013 alignment distillation.

1015 In contrast, assuming a pre-aligned LLM simplifies our framework: the Ref-Teacher can be trained
 1016 without updating the refusal feature or even be replaced by an existing safety-aligned model. Thus,
 1017 while our main experiments target the more challenging scenario, our framework can be naturally
 1018 extended to settings with pre-aligned models.

1019 Moreover, pre-aligned LLMs are also not immune to safety degradation when directly finetuned
 1020 on user data. Preventing this degradation again requires jointly finetuning on safety and user data,
 1021 which also creates the gradient conflict. Therefore, a conflict-mitigation framework such as ours is
 1022 needed even when starting from instruct models.

1023 Therefore, to verify this, we evaluate all methods on Llama3-8B-Instruct. Since alignment-stage
 1024 baselines cannot be applied, we compare only finetuning- and post-finetuning-stage methods. As
 1025 shown in Table A8, our framework that adopting a pre-aligned LLM as Ref-Teacher achieves the
 lowest harmfulness score while preserving strong functional accuracy. Moreover, training the in-

1026 Table A9: Performance comparison across different jailbreak attacks during finetuning. The GCG
 1027 attack (Zou et al. (2023)) is generated using 100 samples from the BeaverTails dataset (Ji et al.
 1028 (2023)), and the AutoDAN attack (Liu et al. (2023)) is generated using 520 samples from the Ad-
 1029 vBench dataset (Zou et al. (2023)). The results demonstrate the strong safety alignment and gen-
 1030 eralization capability of our Ref-Teacher-guided finetuning strategy, which consistently outperforms
 1031 all baselines.

Methods	BeaverTails (Ji et al. (2023))		GCG (Zou et al. (2023))		AutoDAN (Liu et al. (2023))		Average	
	HS ↓	FA ↑	HS ↓	FA ↑	HS ↓	FA ↑	HS ↓	FA ↑
SFT	16.7	40.6	36.0	40.6	69.6	40.6	40.8	40.6
Repoise (Rosati et al. (2024))	30.4	38.4	46.0	38.4	68.5	38.4	48.3	38.4
Vaccine (Huang et al. (2024d))	4.8	24.4	16.0	24.4	18.3	24.4	10.4	24.4
Booster (Huang et al. (2024c))	5.9	43.4	10.0	43.4	37.1	43.4	17.7	43.4
LDIFS (Mukhoti et al. (2023))	4.0	17.0	4.0	17.0	61.9	17.0	23.3	17.0
Lisa (Huang et al. (2024b))	5.3	38.3	52.0	38.3	41.5	38.3	32.9	38.3
Ref-Teacher (Ours)	0.5	49.0	6.0	49.0	0.9	49.0	2.5	49.0

Table A10: Effects of applying Ref-Teacher-guided finetuning to alignment-stage solutions.

Methods	HS ↓	FA ↑
SFT	16.7	40.6
SFT+Ref-Teacher	1.1	42.1
Repoise (Rosati et al. (2024))	30.4	38.4
Repoise+Ref-Teacher	1.4	39.2
Vaccine (Huang et al. (2024d))	4.8	24.4
Vaccine+Ref-Teacher	2.2	22.0
Booster (Huang et al. (2024c))	5.9	43.4
Booster+Ref-Teacher	1.9	43.8

1053 struct model as a Ref-Teacher further enhances safety. These results confirm that our approach re-
 1054 mains effective not only for base models but also for pre-aligned models, offering additional safety
 1055 benefits.

C.4 ROBUSTNESS AGAINST ADVANCED JAILBREAKING ATTACK

1058 When jailbreaking LLMs, advanced techniques such as GCG (Greedy Coordinate Gradient)¹ (Zou
 1059 et al. (2023)) and AutoDAN (Automatically generating DAN-series-like jailbreak prompts)² (Liu
 1060 et al. (2023)) can be used to induce harmful responses beyond simply prompting with harmful
 1061 queries. These methods demonstrated a high attack success rate in eliciting harmful responses,
 1062 even from safety-aligned models, compared to direct harmful prompts. To evaluate the robust-
 1063 ness of our Ref-Teacher-guided finetuning strategy against such advanced jailbreaking attacks, we
 1064 measure harmful score under both GCG and AutoDAN attacks, targeting Llama3-8B-Instruct in a
 1065 black-box setting. While all methods show increased harmful scores under these advanced attacks,
 1066 Table A9 demonstrates that our Ref-Teacher-guided finetuning method is more robust than baseline
 1067 approaches. Notably, although the LDIFS method achieves a low harmful score under the GCG at-
 1068 tack, it suffers from poor finetuning accuracy and exhibits a high harmful score under the AutoDAN
 1069 attack, supporting its impracticality. In contrast, our method maintains both a low harmful score and
 1070 high finetuning accuracy under both GCG and AutoDAN attacks, demonstrating its effectiveness in
 1071 providing reliable protection against increasingly sophisticated jailbreak attempts.

C.5 REINFORCING ALIGNMENT-STAGE SOLUTIONS WITH REF-TEACHER-GUIDED FINETUNING STRATEGY.

1075 To identify whether our Ref-Teacher-guided finetuning strategy can further enhance the safety and
 1076 user-specific task performance of safety-aligned models from alignment-stage techniques, we apply
 1077 our method to these aligned models during finetuning stage and measure both the harmful score

¹<https://github.com/GraySwanAI/nanoGCG>

²<https://github.com/SheltonLiu-N/AutoDAN>

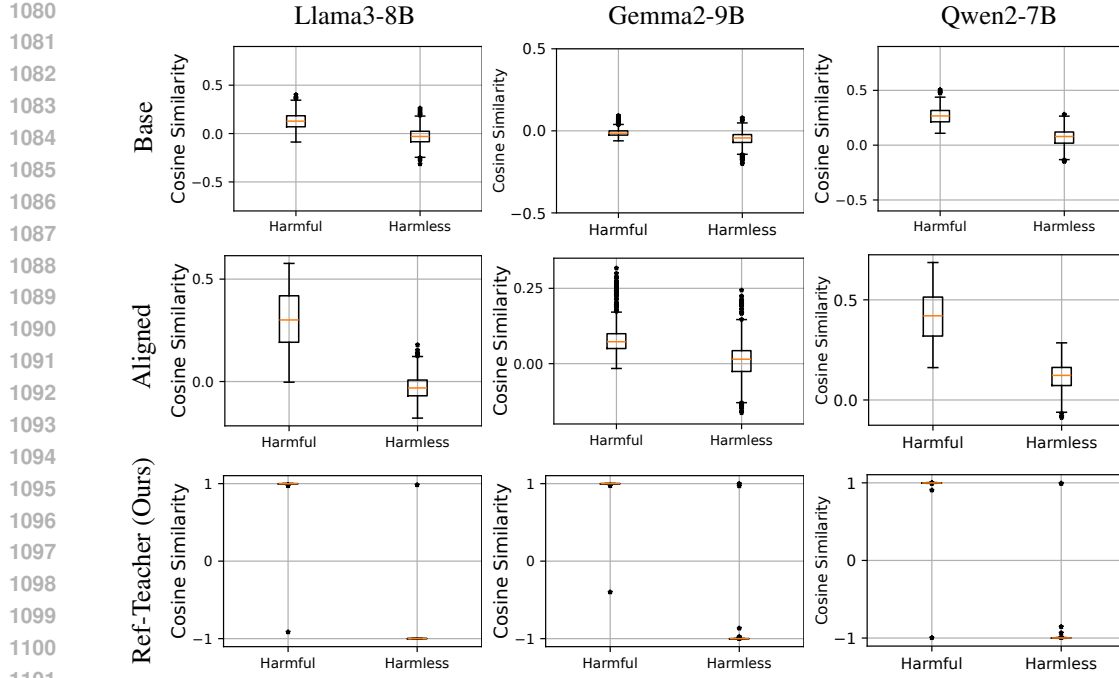


Figure A3: Box plot of cosine similarity distributions for harmful and harmless prompts in the base model, aligned model, and Ref-Teacher (Ours). Prompts were sampled from the BeaverTails (harmful, $n=500$) and Alpaca (harmless, $n=500$) datasets, representing diverse general prompts. The sampled prompts visualized here were excluded from the Ref-Teacher training set. This visualization highlights that safety-alignment introduces the capability to distinguish harmful from harmless prompts.

Table A11: Accuracy of classifying prompts using refusal features. Prompts with cosine similarity above the threshold are classified as harmful, while those below are classified as harmless.

Model	Threshold	Harmful Acc	Harmless Acc	Total Acc
Llama3-8B	0.34	86.0%	78.8%	82.4%
Llama3-8B-Instruct	0.06	95.2%	93.6%	94.4%
Llama3-8B-Ref-Teacher	0.97	99.8%	99.8%	99.8%
Gemma2-9B	-0.037	87.8%	61.2%	74.5%
Gemma2-9B-Instruct	0.035	90.4%	70.4%	80.4%
Gemma2-9B-Ref-Teacher	0.97	99.8%	99.6%	99.7%
Qwen2-7B	0.15	97.6%	88.8%	93.2%
Qwen2-7B-Instruct	0.24	93.2%	97.2%	95.2%
Qwen2-7B-Ref-Teacher	0.9	99.8%	99.6%	99.7%

(HS) and finetuning accuracy (FA). As shown in Table A10, our approach significantly reduces the harmful score while maintaining comparable finetuning accuracy in most cases. The reinforced safety-alignment demonstrates that Ref-Teacher-based data filtering and alignment distillation can complement the alignment-stage solutions. However, the performance of this setting remains inferior to our finetuning framework, highlighting the importance of directly finetuning the base model under Ref-Teacher guidance.

D SAFETY ALIGNMENT ENDOWS MODELS WITH REFUSAL-BASED HARMFULNESS DETECTION

Safety-aligned LLMs tend to exhibit distinct response behaviors as input prompts vary in harmfulness, and this tendency is reflected in their refusal feature, which can serve as a signal for harmfulness classification. While base models can sometimes provide a weak discriminative signal, we observe that this property is more pronounced and reliable in safety aligned models.

To validate this hypothesis, we measure the cosine similarity between the feature of each input prompt and a refusal feature in both base and safety-aligned models, and then assess whether harm-

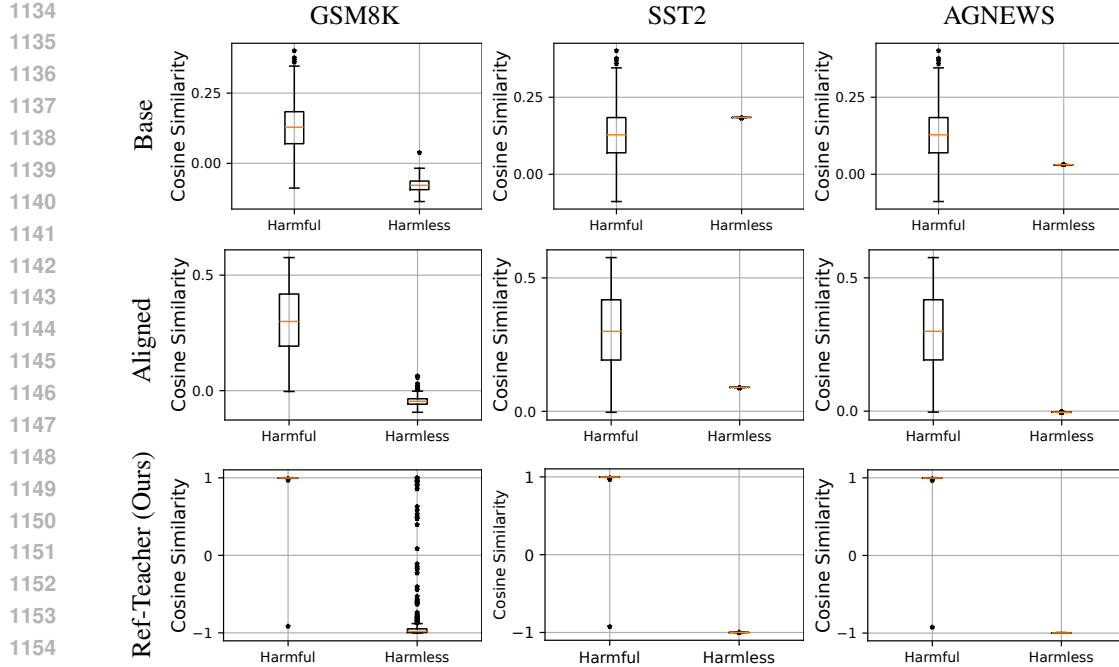


Figure A4: Box plot of cosine similarity distributions for harmful and harmless prompts, evaluated on the base model, aligned model, and Ref-Teacher (Ours). Harmful prompts were sampled from the BeaverTails dataset ($n = 500$), while harmless prompts were sampled from GSM8K, SST2, and AGNEWS ($n = 500$), which are domain-specific downstream task datasets used during the finetuning stage.

Table A12: Classification accuracy using refusal features. Prompts with cosine similarity above the threshold are identified as harmful, and those below as harmless. Thresholds are optimized to maximize total classification accuracy.

Datasets	Model	Threshold	Harmful Acc	Harmless Acc	Total Acc
GSM8K	Llama3-8B	-0.017	95.6%	99.8%	97.7%
	Llama3-8B-Instruct	0.035	98.2%	99.6%	98.9%
	Llama3-8B-Ref-Teacher	0.965	99.8%	99.2%	99.5%
SST2	Llama3-8B	0.190	22.6%	100.0%	61.3%
	Llama3-8B-Instruct	0.095	89.6%	100.0%	94.8%
	Llama3-8B-Ref-Teacher	-0.920	100.0%	100.0%	100.0%
AGNEWS	Llama3-8B	0.032	86.0%	100.0%	93.0%
	Llama3-8B-Instruct	0.010	99.8%	100.0%	99.9%
	Llama3-8B-Ref-Teacher	-0.990	100.0%	100.0%	100.0%

ful and harmless prompts can be separated on the refusal feature. Figure A3 shows the resulting distributions for BeaverTails (harmful) (Ji et al. (2023)) and Alpaca (harmless) (Taori et al. (2023)). Safety-aligned models yield more clearly separated similarity distributions, enabling more reliable discrimination, whereas base models exhibit substantial overlap, though not complete indistinguishability. Numerical results in Table A11 confirm this trend, safety-aligned models achieve higher classification accuracy than the base models for both harmful and harmless prompts.

We further extend the analysis to GSM8K (Cobbe et al. (2021)), SST2 (Socher et al. (2013)), and AGNEWS (Zhang et al. (2015)), which are used during finetuning. Following the same setup as in Fig. A3 and Table A11, we use BeaverTails as harmful data and GSM8K, SST2, and AGNEWS as harmless data with LLaMA3-8B (Llama Team (2024)). Figure A4 reports cosine similarity distributions and Table A12 reports accuracy using the optimal threshold per dataset. Since these downstream datasets are domain-specific and differ from BeaverTails in distribution, the base model shows some separability. Nevertheless, safety-aligned models consistently produce clearer separation and higher accuracy, and Ref-Teacher yields the most distinct separation and the strongest classification performance.

1188 E LIMITATION
11891190 Our Ref-Teacher-guided finetuning framework relies on the Ref-Teacher model, which is trained
1191 using the refusal feature. Consequently, its safety-alignment could be compromised if adversarial
1192 attacks are designed to disrupt or manipulate the refusal feature. In such cases, the customized model
1193 finetuned under the guidance of a compromised Ref-Teacher may also inherit weakened safety-
1194 alignment.1195 F LLM USAGE
11961198 Large Language Models (ChatGPT-5) were used only for improving grammar and clarity in writing.
1199 They did not contribute to research ideation, experimental design, or analysis.
12001201
1202
1203
1204
1205
1206
1207
1208
1209
1210
1211
1212
1213
1214
1215
1216
1217
1218
1219
1220
1221
1222
1223
1224
1225
1226
1227
1228
1229
1230
1231
1232
1233
1234
1235
1236
1237
1238
1239
1240
1241